REPORT SD-TR-85-21

In Search of High J States in the HF (v, J) System

M. A. KWOK, R. L. WILKINS, G. I. SEGAL,
E. F. CROSS, and R. H. UEUNTEN
Aerophysics Laboratory
and
K. L. FOSTER
Space Sciences Laboratory
Laboratory Operations
The Aerospace Corporation
El Segundo, Calif. 90245

14 June 1985

Prepared for
AIR FORCE WEAPONS LABORATORY
Kirtland Air Force Base, N. Mex. 87117

SPACE DIVISION
AIR FORCE SYSTEMS COMMAND
Los Angeles Air Force Station
P.O. Box 92960, Worldway Postal Center
Los Angeles, Calif. 90009

This report was submitted by The Aerospace Corporation, El Segundo, CA 90245, under Contract No. F04701-83-C-0084 with the Space Division, P.O. Box 92960, Worldway Postal Center, Los Angeles, CA 90009-2960. It was reviewed and approved for The Aerospace Corporation by H. R. Rugge, Director, Space Sciences Laboratory and W. P. Thompson, Director, Aerophysics Laboratory. Lt Scott W. Levinson, SD/YNS, was the Air Force Project Officer.

This report has been reviewed by the Public Affairs Office (PAS) and is releasable to the National Technical Information Service (NTIS). At NTIS, it will be available to the general public, including foreign nationals.

This technical report has been reviewed and is approved for publication. Publication of this report does not constitute Air Force approval of the report's findings or conclusions. It is published only for the exchange and stimulation of ideas.

Scott W. Levinson, 2nd Lt, USAF
Project Officer

Joseph Hess, GM-15, Director, West Coast Office, AF Space Technology Center

UNCLASSIFIED

SECURITY CLASSIFICATION OF THIS PAGE *(When Data Entered)*

REPORT DOCUMENTATION PAGE	READ INSTRUCTIONS BEFORE COMPLETING FORM
1. REPORT NUMBER: SD-TR-85-21	2. GOVT ACCESSION NO.: AD-A158 937
	3. RECIPIENT'S CATALOG NUMBER
4. TITLE *(and Subtitle)*: IN SEARCH OF HIGH J STATES IN THE HF(v, J) SYSTEM	5. TYPE OF REPORT & PERIOD COVERED
	6. PERFORMING ORG. REPORT NUMBER: TR-0084A(5603)-2
7. AUTHOR(s): Munson A. Kwok, Roger L. Wilkins, Gary I. Segal, Edward F. Cross, Robert H. Ueunten, and Karen L. Foster	8. CONTRACT OR GRANT NUMBER(s): F04701-83-C-0084
9. PERFORMING ORGANIZATION NAME AND ADDRESS: The Aerospace Corporation, El Segundo, California 90245	10. PROGRAM ELEMENT, PROJECT, TASK AREA & WORK UNIT NUMBERS
11. CONTROLLING OFFICE NAME AND ADDRESS: Air Force Weapons Laboratory, Kirtland Air Force Base, New Mexico 87117	12. REPORT DATE: 14 June 1985
	13. NUMBER OF PAGES: 59
14. MONITORING AGENCY NAME & ADDRESS *(if different from Controlling Office)*: Space Division, Los Angeles Air Force Station, Los Angeles, California 90009	15. SECURITY CLASS. *(of this report)*: Unclassified
	15a. DECLASSIFICATION/DOWNGRADING SCHEDULE

16. DISTRIBUTION STATEMENT *(of this Report)*

Approved for public release; distribution unlimited.

17. DISTRIBUTION STATEMENT *(of the abstract entered in Block 20, if different from Report)*

18. SUPPLEMENTARY NOTES

Yields

19. KEY WORDS *(Continue on reverse side if necessary and identify by block number)*

Collisional Energy Transfer
Energy Transfer
Hydrogen Fluoride Energy Transfer
Hydrogen Fluoride Kinetics
Molecular Energy Transfer
Reactive Flows
Rotational-Rotational Energy Transfer
Vibrational-Rotational Energy Transfer

20. ABSTRACT *(Continue on reverse side if necessary and identify by block number)*

Populations in high rotational states of HF far from rotational-translational equilibrium have been observed in reactive fast flows in a large diameter flow tube. The high rotational states are assumed to be produced from the chemically generated, vibrationally excited HF(v, J) by direct V → R intramolecular energy transfer collisions with ground-state H_2, HF, or Ar species. In a chemical kinetic analysis it is shown that the

cont'd

DD FORM 1473 (FACSIMILE)

UNCLASSIFIED

SECURITY CLASSIFICATION OF THIS PAGE *(When Data Entered)*

19. KEY WORDS (Continued)

20. ABSTRACT (Continued)

results are consistent with the multiquantum V + R energy-transfer mechanism for HF(v, J) + M proposed by R. L. Wilkins for HF(v, J) + HF and D. L. Thompson for HF(v, J) + Ar. Experimental studies are made by monitoring HF R-R spectral emissions between 9 to 22 μm with a sensitive bolometer.

Originator Supplied Keywords include:

PREFACE

Thanks to Drs. L. Wilson and N. Cohen for continuing interest in this work. Special thanks also to J. Narduzzi for assistance with the liquid helium system and L. Goulston and L. Hammond for typing the manuscript.

CONTENTS

FIGURES

TABLES

I. INTRODUCTION

In 1977, Wilkins[1] proposed V → R processes for collisions of initially internally excited HF molecules with target vibrationally unexcited HF molecules. In a V → R process the vibration energy of an initially vibrationally excited HF molecule is transferred into rotational energy of the same HF molecule by an intramolecular energy-transfer mechanism. The interconversions of one or more quanta of vibrational energy into rotational energy produce HF molecules in very high rotational states. The V → R mechanism is enhanced by the close resonance in energy between the rotational levels of the different vibrational states. There are practically no changes in the internal energy states of the target vibrationally unexcited HF molecules. A typical near-resonant V → R process is

$$HF(v_1 = 1,\ J_1 = 3) + HF(v_2 = 0, J_2) \rightarrow HF(v_1' = 0,\ J_1' = 14) + HF(v_2' = 0, J_2' = J_2)$$

$$\Delta E = 26.9\ cm^{-1} \qquad (1)$$

which shows the near-resonance that exists in a high rotational state. This high rotational state nearly matches in energy the low rotational energy of the next higher vibrational state in the HF molecule. The intramolecular energy transfer mechanism leads to the prospect of similar behavior for collisions of internal excited HF species with any chaperone M.

The experimental evidence for this V → R intramolecular mechanism is, to date, somewhat circumstantial. There have not been any HF studies to our knowledge in which the V → R process has been verified unambiguously by an analysis of product states. Possible support for a multiquantum V → R relaxation process is the pulsed HF rotational lasing from very high rotational states of HF first reported by Deutsch.[2] Rotational laser emission from high rotational states of HF has been observed in several studies.[3-11] The V → R mechanism has been shown to be especially efficient for hydrides.[12-14] Krogh and Pimentel and other coworkers have contended that a V-R mechanism of the

proposed nature is an integral part of the explanation of their observed lasing. However, the exoergicity of reactions producing excited HF in all these cases is sufficiently large that one cannot rule out the direct chemical production of an inverted high HF state.

The evidence for the expected V-R behavior with any chaperone is also indirect. Bott[15] has noted that the scaling of quenching coefficients of DF(v) follows an empirical power law v^n, in which n does not change for a wide range of chaperones from homonuclear diatomic to general triatomic molecules. The same behavior has been noticed using flow tube methods by Kwok[16] for HF(v) up to v = 6, including monatomic argon as a chaperone, by Poole and Smith[17] and, recently, in a series of papers by Dzelzkalns and Kaufman.[18-19] It can be inferred from these observations that the relaxation in HF or DF proceeds largely by intramolecular energy exchanges during collision, although the absolute cross sections for V → R energy-transfer vary.

Early work has not helped to clarify the existence or relative importance of this proposed V-R mechanism. On the one hand, the work of Sirkin and Pimentel[9,10] seems to reinforce the possibilities for this type of V-R transfer. In addition, Hinchen[20] has qualitatively observed departures from Boltzmann equilibrium in high J states of HF(v = 0) while exciting low J states of HF(v = 1) using the double resonance technique. He has also observed an enhancement of HF(v = 2) while pumping HF(v = 1) high J states. This occurrence might be caused, in part, by the reversed R-V pathways of the class of proposed mechanisms.

On the other hand, Douglas and Moore,[21] Lampert[22] et al., and Jurisch[23] et al. have now reported that the quenching of at least high v levels of HF occurs predominantly with single vibrational quantum processes with apparently no substantial flow of energies to high J states. It is not clear in such quenching experiments the proportion of mechanisms which are V-V or V-R, V-T type processes. Wilkins' proposal would suggest that, for high v states of HF, the production of high J states and the existence of multivibrational quanta collisions should be intimately related to V-R transfer.

A more detailed discussion of these arguments, pro and con, is stated in a survey by Cohen et al.,[24] which examines rotational relaxation in the HF systems.

We have developed an experiment to detect the presence of high J states out of rotational equilibrium. This experiment is based on steady flow methodologies, which provide good sensitivities and good signal to noise in emission signals, even at very low densities of emitting species. We were attracted to this approach by the availability of a very high detectivity, D*, long wavelength, slow response bolometer, which enables us to observe the high J states of the v = 0 HF manifold via rotational emissions. The lowest v = 0 state manifold provides a "footprint," a unique, nonequilibrium density distribution of J states, to test if the proposed V → R mechanisms are dominant.

In 1978, we reported observing the very high J states.[25] Since then, the work of Hinchen[20] and the work of Haugen, Pence, and Leone[26] have been done. The double resonance work of Haugen et al. suggests that there may, indeed, be an experimental basis for supporting the production of high J states by V-R transfer. Recent calculations by Thompson[27] using a quasi-classical trajectory method on the HF + Ar system helped to clarify our understanding of experimental observations and the relative roles of V-R and R-T processes at the high J states.

II. KINETIC CONSIDERATIONS

The experimental consequences of Wilkins' V-R mechanism proposal can be examined. One prediction is the nearly resonant nature of collisional energy transfer. This means that an HF(v = 1, J = 2) or HF(v = 1, J = 3) should relax to the v = 0 vibrational level by preferentially populating J states that contain sufficient rotational energy to meet this condition. The J = 10-15 states of the v = 0 vibrational state should be enhanced, with the strongest excitation at J = 14. The point is illustrated in Fig. 1, an energy level diagram of HF. Similar vibrational relaxations by one quantum might be expected at higher v's. The proposal also states that multivibrational quanta relaxation mechanisms are probable. Hence, an HF(v = 2, J = 2) might selectively produce an HF(v = 0, J = 18), and so on.

An initial expectation in our experimental planning was that the density distribution of v = 0 high J states would provide a characteristic "footprint" of this near-resonant behavior. The v = 0 states are interesting because there is no lower v state to which further V-R relaxation can occur. The early work of Hinchen and Hobbs[28] indicated that R-T transfer processes (and perhaps R-R processes) might be expected to be slower at high J states. Rapid rotational equilibration should not occur to totally obliterate features of the collisionally induced distribution. With proper experimental conditions, the prospect of R-V processes and of radiative decay were thought to be controllable. A goal of the experiment is then to observe low density high J states of HF in v = 0 manifold.

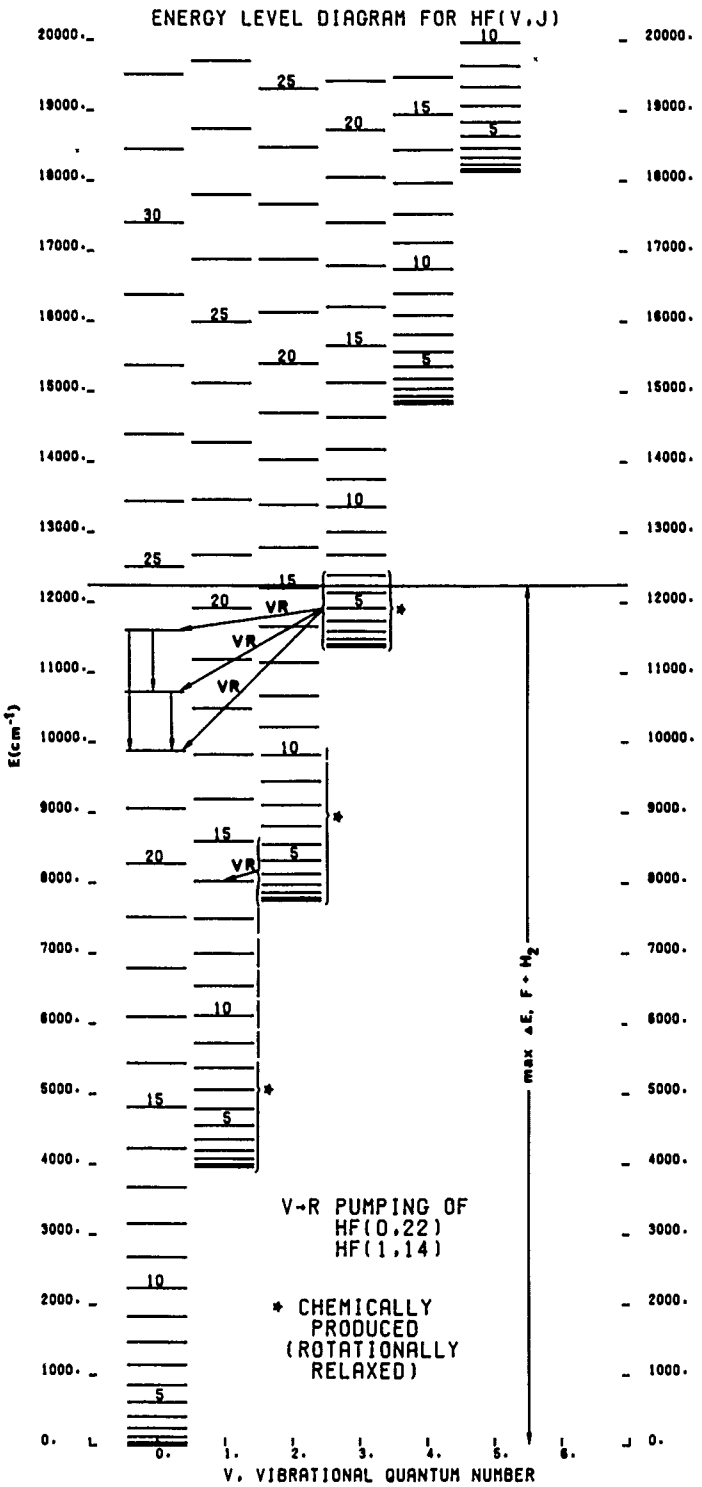

Fig. 1. Energy Level Diagram of HF with F + H_2 Combustion Limits and Pumping Processes for High J States

III. EXPERIMENT

To develop the technique of monitoring the low density high J states, the fast flow, large diameter flow tube facility[16,29] has been modified for the detection of high rotational states in the v = 0 manifold by observing their spontaneous emissions (Table 1). The strategy of detection by emissions rather than by resonance absorptions in a laser technique permits the study of very high J states not conveniently accessible to a probe laser.[20,26,28] Observation of v = 0 high J states then requires the detection of rotational-rotational spontaneous emissions with wavelengths around 10 μm and beyond. Specifically, these studies explore the emission region between 10 and 20 μm. Such long wavelength rotational emissions tend to favor the higher J states since the spontaneous emission coefficients have a $\sim J^3$ dependence (Appendix A). However, at very high J states (above J = 25 and below 10 μm wavelength) radiative decay may become a dominant factor at the characteristic flow times of milliseconds.

Fortunately, a highly sensitive detector in this long wavelength regime is available. A liquid helium (4 K) cooled, gallium-doped germanium bolometer[30] (Infrared Laboratories, Inc.) with a cooled, focusing field mirror, and a cooled, five position filter wheel has been used in this work. For some of the calibration measurements, an internally cooled chopper at 50 Hz, and the built-in preamplifier are also used. In this configuration, a responsivity around 3×10^2 vW^{-1} and an equivalent detectivity, D* of 10^{11} $cm\text{-}Hz^{1/2}\text{-}W^{-1}$, could be achieved in calibration with a cold plate over the KBr window. The field of view is f/6. The bolometer is characteristically slow with 0.59 of the DC response at 50 Hz modulation.

In our studies, the bolometer system is simply mounted on the flow tube, centered on the diameter, transverse to the flow, such that the flow is minimally disturbed. The small amount of highly diluted, chemically produced HF did not degrade noticeably the KBr window over several months. The arrangement is schematically depicted in Fig. 2. Opposite the bolometer, cold fingers had been devised to minimize the effects of the 300 K background

Table 1. HF Spectroscopic Summary

	λ (micron)	A (sec-1)[a]
Rotational Line		
1,14	18.8012	80.000
0,22	11.1696	340.00
Vibrational-Rotational Line		
1P(1)	2.5507	193.03
1P(15)	3.1125	106.05
1R(0)	2.4993	61.40
1R(1)	2.4758	71.68
1R(2)	2.4537	74.50
1R(3)	2.4330	74.74
1R(4)	2.4137	73.71
1R(5)	2.3957	71.96
1R(13)	2.2964	48.10
2P(1)	2.6668	328.70
2P(3)	2.7275	223.81
2P(4)	2.7605	205.17
2P(5)	2.7952	198.50
2P(6)	2.8319	195.53
2P(7)	2.8705	194.01
2P(8)	2.9112	193.07
2R(4)	2.5299	123.63
2R(5)	2.5040	120.25
2R(6)	2.4866	116.04
3P(1)	2.7902	412.45
3P(2)	2.8213	281.39
3P(3)	2.8542	258.39
3P(4)	2.8890	250.34
3P(5)	2.9257	246.89
3P(6)	2.9645	245.20
Band Decay Rates		
1 - 0	2.5242	189.00
2 - 1	2.6389	320.90
2 - 0	1.2902	23.10
3 - 2	2.7609	401.80
3 - 1	1.3493	66.40
3 - 0	0.8793	1.20

[a]J. M. Herbelin and G. Emanuel, J. Chem. Phys. 60, 689 (1974), see also Appendix A.

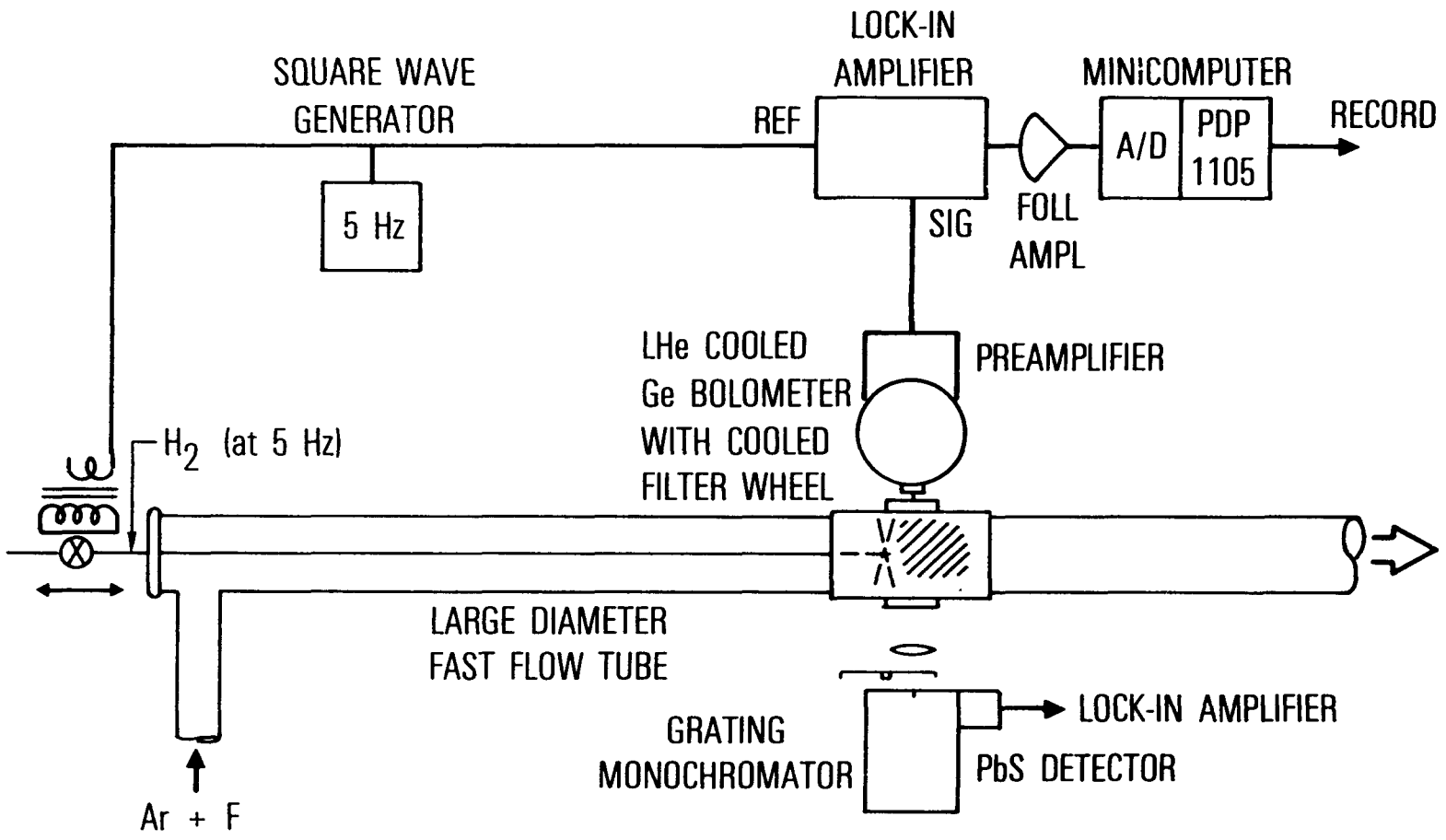

Fig. 2. Experimental Schematic

radiation. These were not needed because an alternative technique of distinguishing true signals from background was successful. By following a technique suggested by Benard,[31] one of the reagents of the flow can be modulated at a slow frequency, 5 to 10 Hz. This in turn modulates the product HF emission. The HF is produced by the reaction F + H_2 in a manner previously described.[29] In this work, the H_2 is modulated before passage through the movable injector by an oscillating solenoid valve (Skinner), which could, after considerable adjustments with carrier argon, produce a nearly 100% modulation with a credible initial square wave in the emission. The Skinner valve itself is driven by a 5-Hz amplified square wave, which also provides the reference frequency for the lock-in amplifier.

The bandwidths of spectral filters used at the 10 to 20 μm wavelength region are depicted in Fig. 3. In most cases, manufacturer traces of the transmittances were available at liquid helium and at room temperature. The principal narrowband filters of interest are Nos. 4 and 6. Data are reported from No. 2 whereas No. 5 broke in early use. In addition, a filter with a transmittance curve at 2.6 to 2.9 μm wavelength is used on the wheel. This filter is instrumental in correlating the absolute number densities of HF(v, J) states with bolometer signals.

A calibration of the bolometer system responsivity has been made. For these tests, five of the six listed filters were used as well as a built-in preamplifier system not used in the flow tube studies. The system is linear up to 2.5×10^{-5} W on the detector, regardless of filter wavelength, with a responsivity of 308 ± 30 vW^{-1} determined from the straight line slope (Appendix B).

For these experiments to be successful, the optical attenuation on the wings of the narrowband filters must be sufficient. The filters used are designed to block undesired radiation to better than 5×10^{-4} from the ultraviolet to the infrared. The relevant radiation is further discriminated from stray radiation by the modulation technique already described. This leaves radiation, which is part of the reacting flow itself. This optical attenuation property has been verified on several of the long wavelength

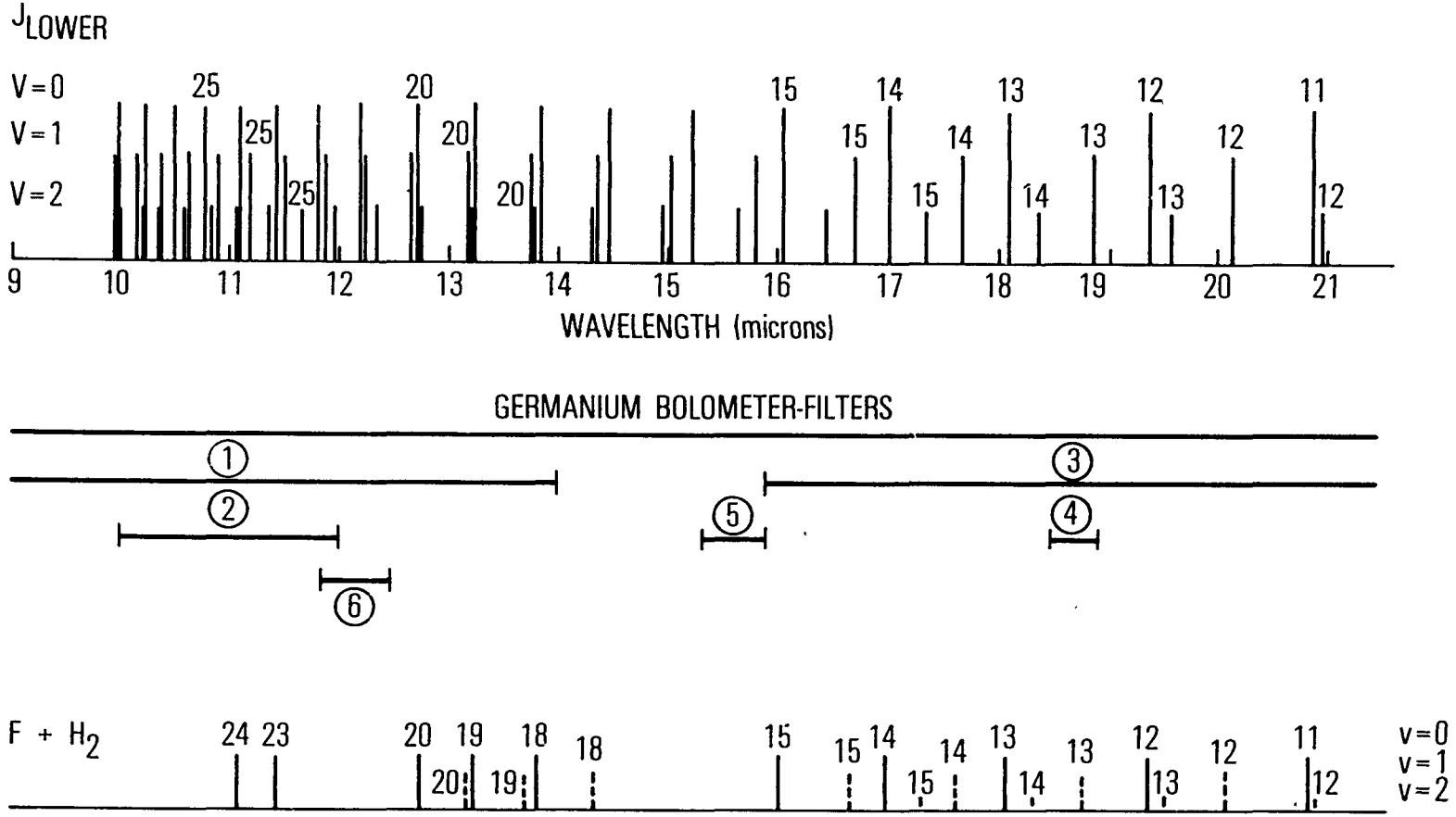

Fig. 3. Long Wavelength Filter Bandwidths. Top graphic shows HF rotational line positions for v = 0, tallest lines; v = 1, medium lines; and v = 2, shortest lines. Middle graphic shows the bandwidths. Bottom graphic suggests the "footprint" distribution of rotational emissions for a $F + H_2$ reaction.

filters, including filter No. 2 (10.0 to 12.1 μm) and No. 4 (18.5 to 18.9 μm) at the most probable wavelength location for the strongest undesired chemiluminescence, namely the HF vibrational-rotational fundamental emissions at 2.3 to 3.3 μm.

As subsequent density estimates show, blockage on wings needed to be $O(10^{-4})$ or better to suppress this radiation. This emission was simulated by blackbody radiation and a 2.6 to 2.9 μm filter with approximately 90% transmission over the bandwidth and the same severe optical attenuation elsewhere. As one ranged the blackbody radiance over a factor of 200 in this 2.6 to 2.9 μm bandwidth with the 300 K background as a baseline signal, random changes in signal of less than 5% were observed on filter Nos. 2 and 4 (Appendix B). From these data it was concluded that the optical attenuation on the shorter wavelength side is probably much better than 2.5×10^{-4} on such long wavelength narrowband filters. An additional test using cw HF laser $P_2(8)$ (2.911 μm) radiation, which was intensity modulated at lock-in amplifier frequencies, showed the attenuation to be even much better than 2×10^{-5} on filter Nos. 2, 4, and 6. The attenuation exceeded our capabilities to detect it because of uncertainties from detector and amplifier noise.

Data acquisition was assisted by the use of a PDP 11/10 minicomputer system. The computer performed digital filtering on the lock-in amplifier output signal and executed real-time running signal averages on this signal (Appendix B). In this case, the lock-in amplifier became simply a narrow-frequency-bandwidth-analog-amplifier performing the first stage of signal processing with some filtering and signal averaging of the very low level signals. The minicomputer also provided a record keeping function and average data tabulations and displays. Histograms of the distribution signal voltages contributing to the average could be provided for specific sampling windows; these diagrams could provide measures of signal uncertainties.

Absolute number densities were determined using methods previously developed[29] involving the grating monochromator in Fig. 2. These data provided sufficient inputs for a kinetic analysis to be described later. They also anchored the bolometric relative intensities in an absolute sense. This

circuitous approach to an absolute bolometer calibration is considered more reliable than that using a standard source because the internal focusing mirror of the bolometer was not manipulated to exactly define the optical volume. With the reasonable assumption that the bolometer responsivity at 2.5 and 10 μm was essentially the same, knowledge of the absolute number densities provides an *in situ* estimate of the radiance on the bolometric detector through the 2.6 to 2.9 μm filter with a specified transmittance curve. In turn, any other signal at long wavelength can then be related to a radiance, and, hence a number density without too much concern for the exact field of view of the bolometer. The approach is acceptable as long as both optical volumes are definitely along the tube diameter, and optical image areas are about the same size and are small compared with tube cross section areas.

IV. RESULTS AND DISCUSSION

The primary results of these studies, as depicted in Figs. 4 and 5, are the observations of detectible HF high J state densities. The deduced absolute number densities indicate that these high J state densities are far from rotational equilibrium. The origins of these species are consistent with V-R,T collisional transfer processes from lower J states at high v quantum numbers. Both the spectral locations of observed rotational emissions and the successful fitting of a simple model to the density results in Figs. 4 and 5 tend to support the V-R,T mechanism. The quenching rate deduced from model results suggests that the dominant quenching mechanism is R-T transfer.

A. STATE IDENTIFICATION

The principal signal-averaged results are depicted in Figs. 4 and 5 for respective relative emissions from filter No. 4, 18 μm wavelength, from filter No. 2, 10 to 12 μm, and No. 6, 11.9 to 12.4 μm. Once the likely emitting states are identified, approximate number densities can be estimated for filter Nos. 4 and 6, as shown in Figs. 4 and 5 using both the 2.6 to 2.9 μm filter signal voltage results shown in Fig. 6 and the absolute number densities shown in Fig. 7. Less than 3% contributions to emissions in Fig. 7 came from v = 4 or higher states. The signals observed with filter Nos. 2, 4, and 6 are also certainly not caused by leakage of vibrational-rotational fundamental or overtone radiations at shorter wavelengths. The shapes as a function of axial position do not resemble those in Fig. 6 for integrated shorter wavelength emissions. From the sideband blockage measurements we conclude that a leakage signal should be at most only on the order of 10^{-5} that of signals in Fig. 6 while, in fact, the actual observed signals are 10^{-3} to 10^{-4} of those in Fig. 6.

As suggested in Fig. 3, the emission through the No. 4 filter is actually centered at 18.8 μm. The most probable transition is v = 1, J = 14 → J = 13 at 18.801 μm near the 0.68 peak of filter transmittance. This means the v = 1, J = 14 state is being monitored with a peak density averaged along tube diameter of over 3×10^9 cm^{-3}. Spectroscopic parameters for long wavelength

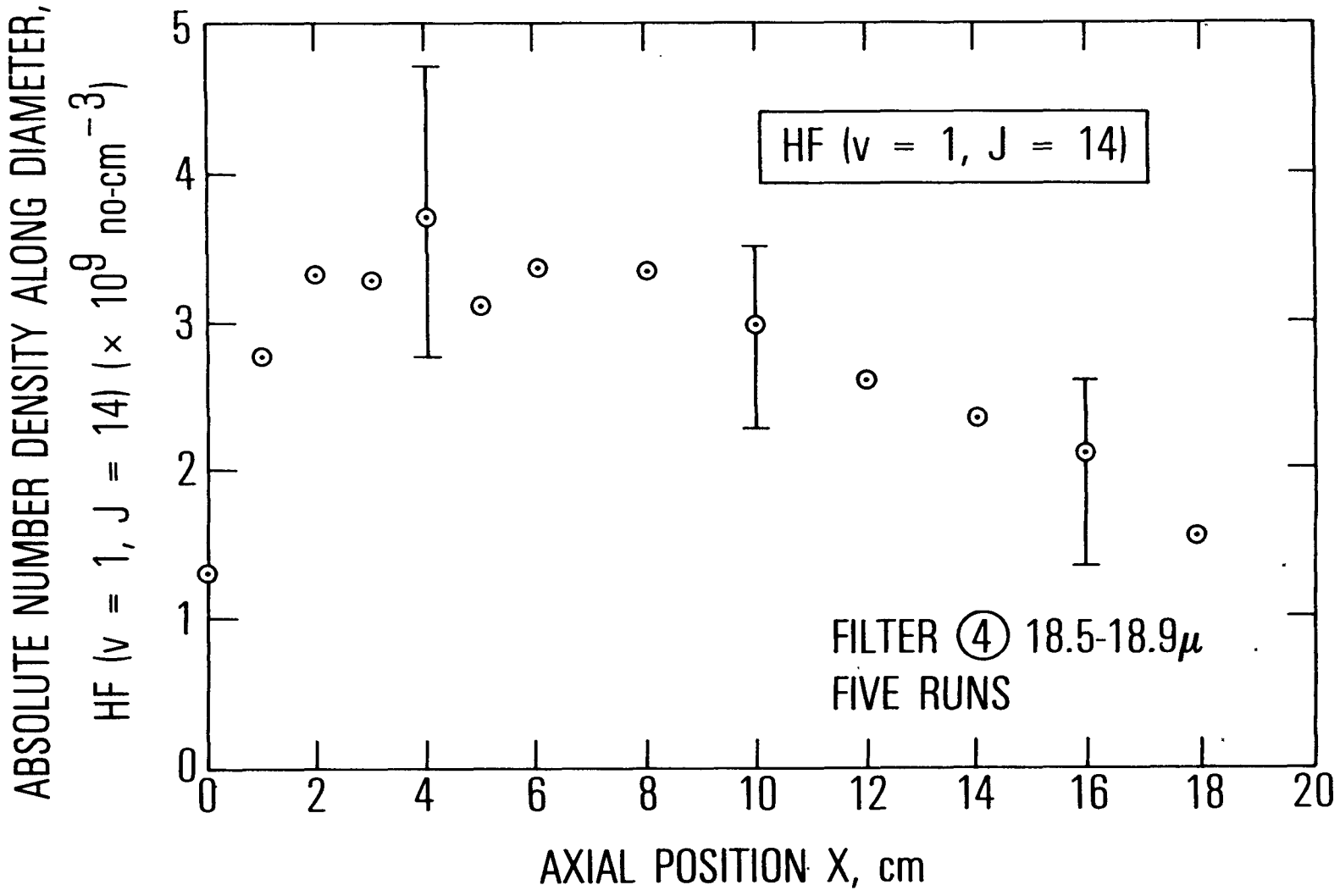

Fig. 4. 18μ Filter Results (with Absolute Density). Number density of HF(v = 1, J = 14) as a function of tube axial position.

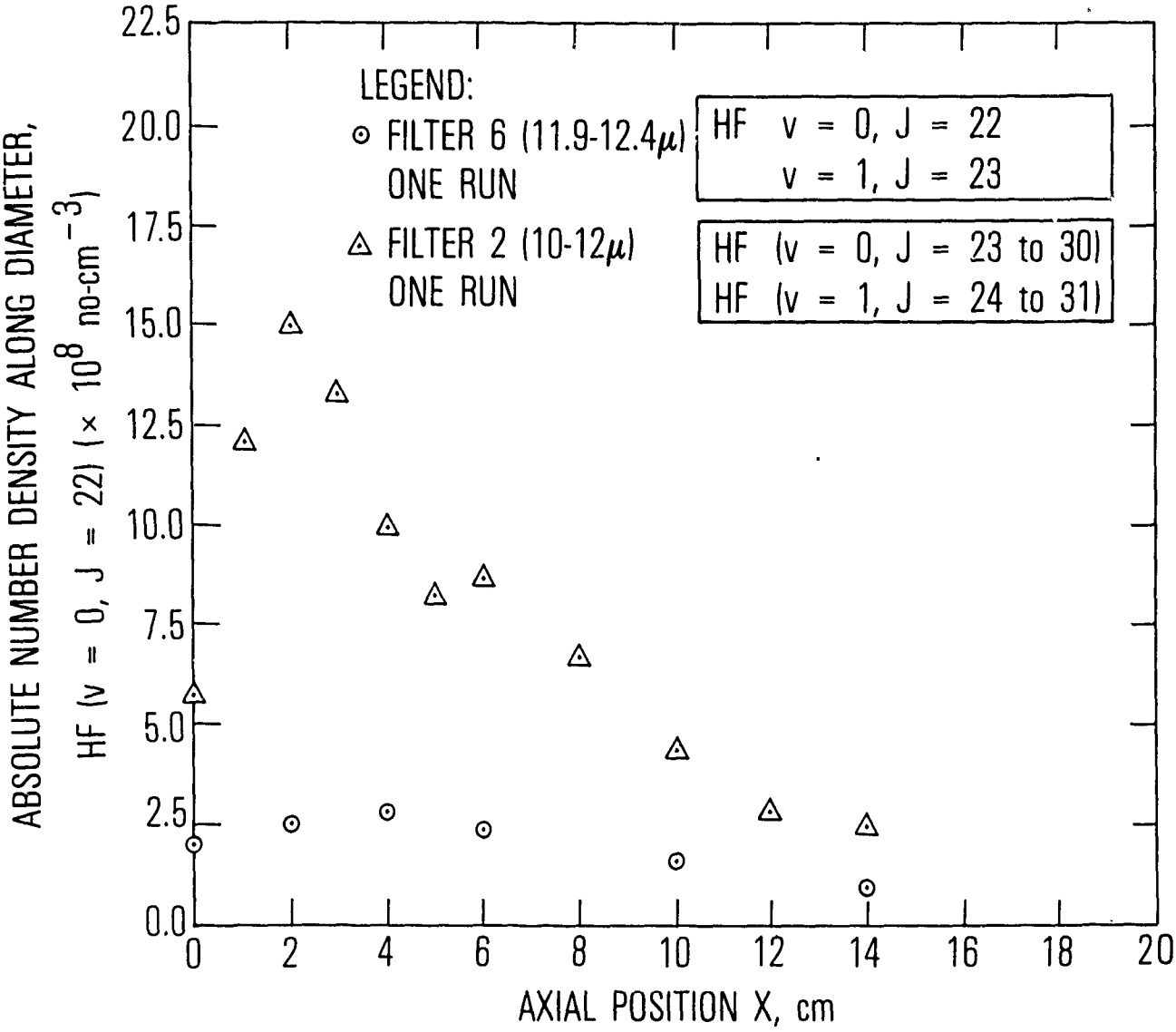

Fig. 5. 12μ Filter Results (with Absolute Density). Number density of HF(v = 0, J = 22) as a function of tube axial position from calibrated results of filter 6. Filter 2 shows, on a relative basis, more emissions from J states higher than J = 22.

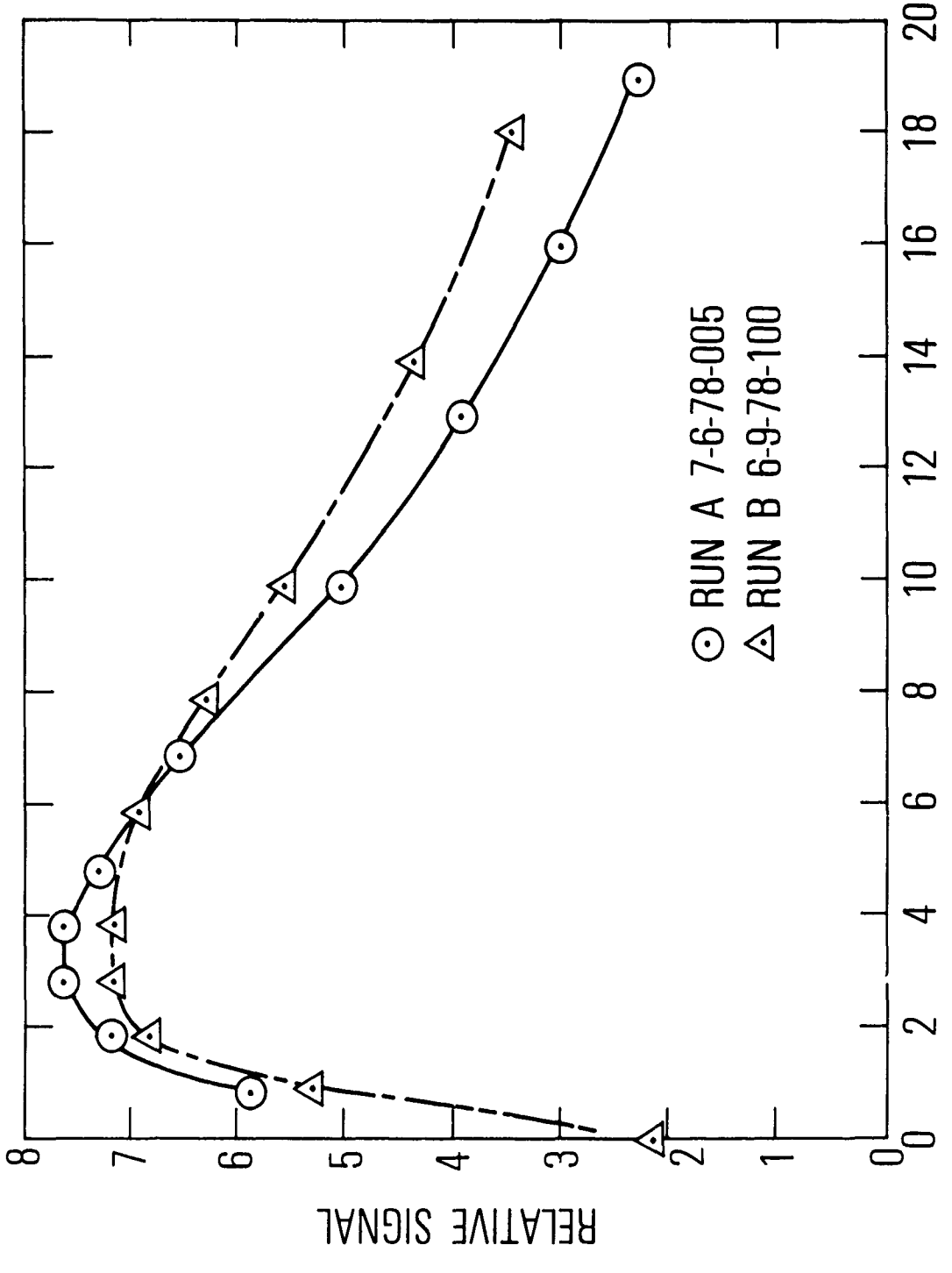

Fig. 6. 2.6 to 2.9 Filter Results

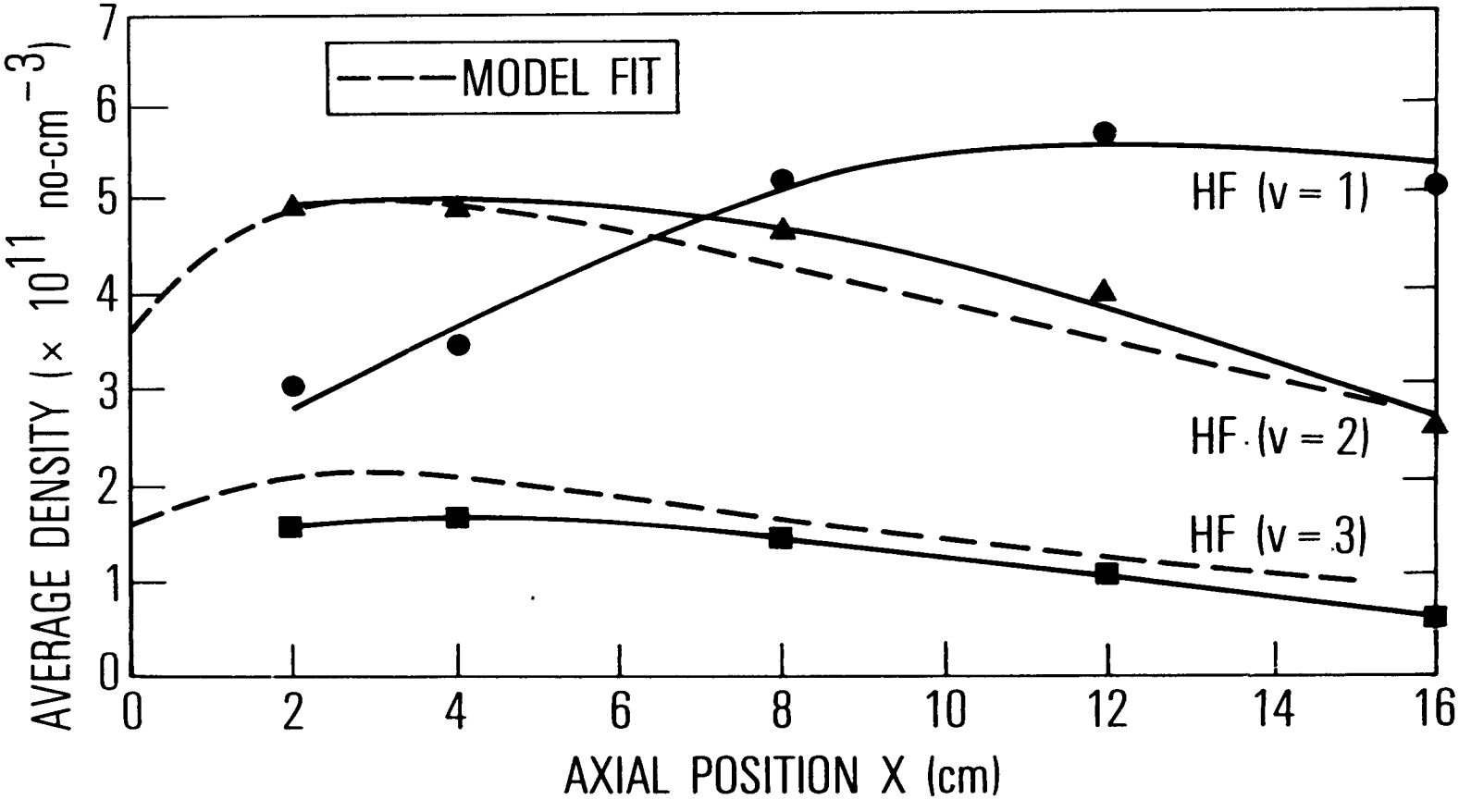

Fig. 7. Absolute Number Densities. v = 1, 2, 3 at low J (with model fits) for Boltzmannized lower J states. Model results are from model described below.

lines are shown in Table 1. The next nearest spectral lines are v = 0, J = 13 → J = 12 at 19.369 μm; v = 2, J = 15 → J = 14 at 18.363 μm; and v = 3, J = 15 → J = 14 at 19.113 μm. With a bandwidth of 0.55 μm, the next nearest line position for v = 3, 15 → 14 has a transmittance no more than 0.24 and the others, less than 0.05. Assuming the intensities of higher v lines to be probably equal or less, the likelihood of observing predominantly the v = 1, J = 14 state is large. Both the estimated absolute number density and the differences in axial variations of the Boltzmannized low J, v = 1 densities, and the J = 14 density suggest large rotational nonequilibrium effects. Even on this time scale of a millisecond the effects of rotational nonequilibrium have not been relaxed. As shown in Table 2, density of the v = 1, J = 14 state was six orders of magnitude larger than that predicted for a Boltzmann distribution.

Similar predictions can be made for the observations with filter Nos. 6 and 2 (Fig. 5). Filter No. 2 covers wavelengths including emissions from v = 0, J ≈ 23 - 29; v = 1, J = 24 - 31; and v = 2, J > 26. The limited exoergicity of reaction F + H_2 would tend to make emissions from such very high J states of v = 3, 2, and 1 extremely unlikely even after any collisional redistribution or relaxation of initial produce energies. Therefore, the filter emissions most likely represent v = 0, J > 23 states. It is interesting to note that observable densities are recordable at these high J states, obviously far out of Boltzmann equilibrium. By the same token, the signals from much narrower filter No. 6 must be from two possible states: v = 0, J = 22 or v = 1, J = 23 with the transition from the former state much more probable. The number density can be estimated to be around 3×10^8 no-cm^{-3}, some four orders of magnitude smaller than the total amount of HF produced. In Table 2, the displacement out of Boltzmann equilibrium is severe even if one conservatively assumes the undetected HF(v = 0) density to be about equal to that of HF(v = 2).

B. ORIGIN OF HIGH J STATE SPECIES

The central question is the nature of production of these very high J species. From the axial variations, which correlate with the combustion zone for F + H_2, one can propose that these species are either produced directly in

Table 2. High J Densities Compared to Boltzmann

	(T = 295 K, P = 1 Torr)		
	Observed	Boltzmann Factor	Ratio
$N(v = 1, J = 14)/N(v = 1)$	6×10^{-3}	9×10^{-9}	7×10^{5}
$N(v = 0, J = 22)/N(v = 2)$	5×10^{-4}	1×10^{-20}[a]	$0(10^{16})$

[a] Assume approximately equal to $[N(v = 0, J = 22)/N(v = 0)]$

the chemical reaction or they are produced by one or several collisional relaxation steps following the reactive production of HF at other vibrational rotational states. The possible maximum J states, which can be produced reactively for a 34.7 kcal-mol^{-1} exothermicity of reaction,[32] are illustrated in Fig. 1. The maximum J's are not substantially changed when the other components to exoergicity are included. For v = 0, 1, 2, and 3 the maximum J states that can be thermodynamically produced are J = 24, 20, 15, and 6, respectively.

For the state v = 1, J = 14, several considerations indicate that we will not be able to distinguish between the two propositions. The information in Fig. 1 suggests that direct production of this state by the reaction F + H_2 is quite feasible. A rate coefficient has been computed by Wilkins[33] using classical trajectory calculations, which are over two orders of magnitude smaller than those for highly produced states. On the other hand, studies of the F + H_2 initial product distribution have not reported the state. Possibly the state is beyond the sensitivity of experiments. Wilkins[1] has also suggested that the state v = 1, J = 14 can be populated by the V-R process

$$HF(v = 2, J = 3) + M \rightarrow HF(v = 1, J = 14) + M \quad \Delta E = 48.2 \text{ cm}^{-1} \qquad (2)$$

These pathways are near-resonant for transfers from the densely populated low J states of v = 2, and in this case produced by chemical reaction and rapidly relaxed to rotational equilibrium on these time scales. The presence of v = 1, J = 14 may indicate that this type of V-R transfer is occurring. It is likely that both types of processes are important in producing v = 1, J = 14. In the analysis discussed in the next paragraph both types of processes are suggested.

It is far less probable that the v = 0, J = 22 state is produced by direct chemical reaction. This state is on the outer edge of the optimistic maximum J regime shown in Fig. 1. If translational energies are considered, the maximum J regime would be lowered. Both experiment[32] and theory[33] demonstrate that the amount of energy apportioned to translation increases significantly with descending vibrational level. Theory[33] predicts absolutely

no F + H_2 initial product distribution in any v = 0 state, but no experiment has been attempted to verify this statement. It is important to note, however, that Sung and Setser[34] consider that rotational products can occur up to the limit of exoergicity. Further, Cohen[24] has noted that even slightly more energy than in defined limits (hypothetically) may be accessible if the translational energies of the tail of a Boltzmann distribution are available.

If direct chemical production is not the main process creating v = 0, J = 22, then one must consider the chemical production of higher v, lower J states followed by collisional relaxation into this state. An examination of the HF energy level diagram in Fig. 1 suggests that the most probable precursor states are in v = 3. By a succession of nearly resonant V-R collisions the internal energy in these states can migrate to high J states in v = 2, and still higher J states in v = 1. Finally the v = 0, J > 24 states can be reached, which in turn can be relaxed to J = 22 by R-R,T rotational relaxation processes.

A v = 3 precursor would be very consistent with data of filter No. 2 case. As the axial variation shows, these very high J states are rapidly produced within the combustion zone. It is unlikely that the density levels and the characteristic time resolution of the flow tube permit stepwise processes of too great a sequential complexity to be observed. It is, therefore, possible that the production of the J = 22 state represents evidence of a V-R process involving nearly resonant multiple vibrational quanta conversions to rotational energy. For the current work such a process in a single step might be

$$HF(v = 3, J = 3) + M \rightarrow HF(v = 0, J = 24) + M \qquad (3)$$

for collision partners M = Ar, H_2, H, or HF. Such processes were also proposed by Wilkins[1] as well as Thompson.[27] (For such a case, the v = 0, J = 22 density is 10^{-3} that of the v = 3 states.) A two-step sequence would still involve one multiple vibrational quanta conversion.

An alternate, less probable set of rotationally relaxed precursor states

could occur at v = 2. To reach v = 0, J = 22, some rapid sequential excitation by R-R,T processes would be needed. Such behavior is common for close lying low J states, and Thompson[27] suggests fast exoergic processes even at high J's with large energy gaps.

Similar support for such V-R mechanisms has been provided by the explorations of Hinchen[20] using the double resonance technique in which no chemistry is involved. The excitation of a v = 1, low J state created measurable densities far out of rotational equilibrium for v = 0, J > 11 states. A high J state density was perhaps 10^{-3} smaller than a lower J HF(v = 1, J) density. Even more recent work by Hinchen, in which a v = 1 high J state such as J = 12 was pumped, led to the appearance of observable densities in v = 2, low J. This behavior suggests the existence of the reverse process R → V. The careful work of Haugen, et al.[26] has reinforced the prospect of V-R mechanisms producing higher J states in these intermediate ranges of J.

The low values of the very high J state densities relative to excited lower J densities seen in this work, in Haugen's work, and in the Hinchen studies, lead to the realization that the sum of the production rates is much smaller than the sum of quenching rates by at least two to three orders of magnitude. This fact can be seen by doing an approximate steady-state analysis in the vicinity of X = 4 cm since all the absolute densities are known. One cannot, however, a priori conclude that the production rates are slow, and, therefore this class of V-R collisional energy transfer processes exists, but is of little importance compared with other V-T mechanisms. Rather, one might predict the V-R production rates are fast if they indeed produce rotational lasing inversions. All the reported pulsed rotational lasing occurs on microsecond time scales for modest pressures. If the production rates are fast, as Wilkins predicts them, the quenching rates for high J densities must be extremely fast relative to the pumping rates.

C. MODEL

A simple analytical model can be devised to assess phenomenological production and quenching rates of these high J states. The experimental parameters useful in a model study are the observed maximum number density,

and the rise and decay slopes of density as a function of axial location of a particular v,J state.

The model uses solutions of uncoupled first order differential equations describing the kinetics in an annular streamtube with radius r. The kinetics reflect the chemical production of a precursor state (or high J state):

$$F + H_2 \xrightarrow{K_p(v_o)} HF(v_o, J_o') + H \tag{4}$$

the phenomenological pumping of a high J state $HF(v_o', J_o'')$ by a V → R energy-transfer process:

$$HF(v_o, J_o') + M_P \xrightarrow{K_p^{VR}} HF(v_o', J_o'') + M_P \tag{5}$$

where J_o' represents a Boltzmannized rotational state and $v_o' = v_o - n$ with $n = 1$, 2, or 3; and the phenomenological collisional quenching

$$HF(v_o, J_o') + M_Q \xrightarrow{K_Q} HF(v_1, J_1) + M_Q \tag{6}$$

and phenomenological radiative quenching

$$HF(v_o, J_o') \xrightarrow{A_{rad}} HF(v_1, J_1) + h\nu \tag{7}$$

For the purely chemically produced state the limiting reagent is F atoms with H_2 in vast excess. The chemically produced state $HF(v_o, J_o')$ is governed by the differential equation determined from Eqs. (4), (6), and (7)

$$U(r)\frac{d}{dX}[HF(v_o, J_o')] = K_p(v_o)[F][H_2] - \left\{K_{Q1}[H_2] + K_{Q2}[Ar] + K_{Q3}[HF] + K_{Q4}[H] + A_{rad}\right\} \bullet [HF(v_o, J_o')] \tag{8a}$$

where U(r) is the velocity at r in the annular streamtube, and

$$[F] = [F]_o \, e^{-\int_{v_o} K_p(v_o)[H_2]\frac{X}{U}} = [F]_o \, e^{-K_p[H_2]\,\frac{X}{U}} \tag{8b}$$

$$[H] = [F]_o \, [1-e^{-K_p[H_2]\,\frac{X}{U}}] \tag{8c}$$

and

$$[HF(v_o, J_o')]_{X=0} = 0 \tag{8d}$$

The dominant quencher is considered radiative decay even in the case of $v_o = 3$. For $v_o = 1$, 2, or 3, the general solution to Eq. (8a) for the annular streamtube of radius r with $HF(v_o, J_o') \equiv N(v_o, J_o')$ becomes

$$N(v_o, J_o') = \frac{R_p(v_o)[F]_o}{[R_F - R_Q(v_o)]} \left\{ e^{-R_Q(v_o)[X/U]} - e^{-R_p[X]/U} \right\} \tag{9a}$$

where

$$R_p(v_o) = K_p(v_o)[H_2] \tag{9b}$$

$$R_p = K_p[H_2] \tag{9c}$$

$$R_Q(v_o) = A_{rad}(v_o) \tag{9d}$$

where $K_p(v_o)$ represents the specific rate coefficient for production of $HF(v_o)$ by the pumping reaction $F + H_2$, Eq. (4); K_p represents the total rate coefficient for production of HF species, see Eq. (8b); and $A_{rad}(v_o)$ is the total radiative decay rate from $HF(v_o)$, see Eq. (7). The solution, Eq. (9a), is expressed as the difference of two exponentials. As rotational equilibrium has been observed to occur on these millisecond time scales with virtually the total vibrational density in the low J states, $J \leq 6$, one can treat this precursor to a high J state as a vibrational density summed over all high density J levels with the same two exponential solutions.

The rate equation for a high J state in the annular streamtube becomes,

$$U(r)\frac{d}{dX}[HF(v_o', J_o'')] = K_p(v_1,J_1)[F][H_2] + \{K_{P1}^{VR}[H_2] + K_{P2}^{VR}[Ar] + K_{P3}^{VR}[HF] + K_{P4}^{VR}[H]\}\bullet[HF(v_o)] - \{K_{Q1}[H_2] + K_{Q2}[Ar] + K_{Q3}[HF] + K_{Q4}[H] + A_{rad}\}[HF(v_o', J_o'')] \quad (10)$$

where [F] and $[HF(v_o)]$ are the specified exponential solutions as a function of X. The chemical pumping term is included to assess the HF(v = 1, J = 14) case. The HF(v = 0, J = 22) is assumed to be not chemically pumped. With the highly nearly resonant nature of V-R, the R-V collisional processes have been decoupled justifiably in this study because of the orders of magnitude differences in densities between $HF(v_o)$ and $HF(v_o', J_o'')$. In addition, statistical weight ratios in the equilibrium constants favor the forward V-R direction by a factor of four or more. To the high J state, the low J precursor states appear as imperturbable reservoirs. Near-resonant processes involving neighboring low density high J states have been similarly neglected because of the dominance of $HF(v_o)$ densities.

Collisional pumping of either the (1, 14) or (0, 22) state is assumed to occur in one step. Stepwise processes such as the cascading of (0, 24) and (0, 23) into (0, 22) are assumed to originate from the same precursor. Then pumping rates in these solutions can be construed as lower bound estimates, since an actual stepwise process would demand faster intermediate steps to attain the observed x or temporal dependence.

The solution to the rate Eq. (10) within the annular streamtube for the high J state will appear as the sum of three exponentials:

$$N(v, \text{high } J) = \frac{R_P^{VR} R_{P(v_o)} [F]_o}{[R_P - R_Q(v_o)]} \left\{ \frac{R_P - R_Q(v_o) + \gamma[R_Q(v_o) - R_Q]\, e^{[-R_Q X]/U}}{(R_Q - R_P)\,[R_Q - R_Q(v_o)]} \right.$$

$$\left. - \frac{[-R_P X]/U}{[(1-\gamma)e]/(R_Q - R_P)} + \frac{e^{[-R_Q(v_o)X]/U}}{[R_Q - R_Q(v_o)]} \right\} \qquad (11a)$$

where

$$\gamma \equiv \frac{R_p(v, \text{high } J)}{R_P^{VR}} \qquad (11b)$$

$$R_p(v, \text{high } J) \equiv K_p(v, \text{high } J)\,[H_2] \qquad (11c)$$

$$R_P^{vR} \equiv K_P^{vR}\{[H_2] + \alpha_1[Ar] + \alpha_2\,[HF] + \alpha_3\,[H]\} \qquad (11d)$$

and

$$R_Q \equiv R_Q(v, \text{high } J) = A(v,J) + K_Q\,[H_2] + \beta_1[Ar] + \beta_2[HF] + \beta_3[H] \qquad (11e)$$

The rate coefficient for direct chemical reaction to the high J state is $K_p(v, J)$, which for (1, 14) we take to be 0.003 K_p and for (0, 22) we take to be zero.[33] Pumping by collisional V-R processes to the state with H_2 chaperone is given by K_P^{VR}, and general quenching by H_2 from that state, by K_Q. Similarly, ratios for coefficients with the other chaperones are denoted by the α_1 and β_i. The radiative decay rates of the state are given by A(v, J) for V-R and R-R spectral emissions.

The chemical pumping specific rate coefficients $K_p(v_o, J_o)$ and the radiative decay rates (Table 1) are assumed known from previous work. All number densities are observed. Velocity U(r) can be estimated from flow measurements, tube pressure, and tube diameter. The unknowns to be determined are

the pumping rate by V-R processes, R_P^{VR}, and the quenching rate, R_Q. If relationships are established for α_i and β_i, the unknowns become K_P^{VR} and K_Q, which are uniquely determined.

The constructions for the α_i and β_i are summarized in Table 3. The α_i for HF and argon chaperones can be established from reported absolute rate coefficients for the HF(v = 1) + M, V-R vibrational relaxation process.[35] The α_i for H as a chaperone can be found by using the absolute rates for HF(v = 1, 2) + H observed by Heidner and Bott.[36,37] The assumption is made that for these vibrational levels, this process behaves like a V-R process. In any case, excitation of high J states by V-R pumping caused by HF and H (and SF_6) is negligible according to the approximate density relationships for Ar, H_2, HF, and H summarized in Table 3. By far the principal pumping chaperone will be argon under our flow conditions with perhaps a 20% contribution from H_2 and 10% from HF. From Wilkins,[1] 11/30 of the HF(v = 3) + M process ends in HF(v = 0), and 24/30 of HF(v = 2) + M in HF(v = 1).

Definition of the β_i for the observed quenching is very different. We assume two patterns for the β_i. In the first, we assume the quench is dominated by V-R and R,T-V processes and thus adopt the same pattern of β_i as that of the α_i. In the second, the pattern is heavily influenced by the calculations of Thompson and will be discussed later.[27] In essence, R-T processes are included, and the dominant quenching process is actually the single J quantum rotational relaxation by the argon chaperone. Thus, the details for the other chaperones are not too critical in case 2.

The pathways for the two models used for the (1, 14) and (0, 22) states are illustrated in Fig. 8. The simulation is completed by integrating the radially dependent solution Eq. (11) along the tube diameter 2R and thus generating an axially dependent average number density along the tube diameter. A paraboloidal velocity profile is assumed in what is designed to be fully developed, laminar flow.[29]

$$\bar{N}(X;\ v,\ \text{high J}) = \frac{1}{R}\int_0^R N(r,\ X;\ v,\ \text{high J})\ dr \qquad (12)$$

It has also been established for this large diameter flow tube that transverse diffusion effects are properly arrested in the first two diameters of study.[29]

Table 3. Scaling for Chaperone

M	Measured $^{35-37}$ V-R HF(v = 1) + M (cm^3-mol^{-1}-sec^{-1})	Ratio	α_i	βi Case 1 V-R	βi Case 2 (R-R,T)	Density ($mol\text{-}cm^{-3}$)
HF	10^{12}	1	100	100	1	$\sim 2.0 \times 10^{-12}$
H_2	10^{10}	10^{-2}	1	1	1	2.3×10^{-10}
H	10^{11}	10^{-1}	10	10	10^{-1}	$\sim 2.0 \times 10^{-12}$
Ar	$<10^8$	$<10^{-4}$	10^{-2}	10^{-2}	10^{-1}	5.4×10^{-8}

V-R scaling for v > 1 is assumed to proceed by a $v^{2.7}$ dependence and to be apportioned for multiple v processes as reported by Wilkins.[1]

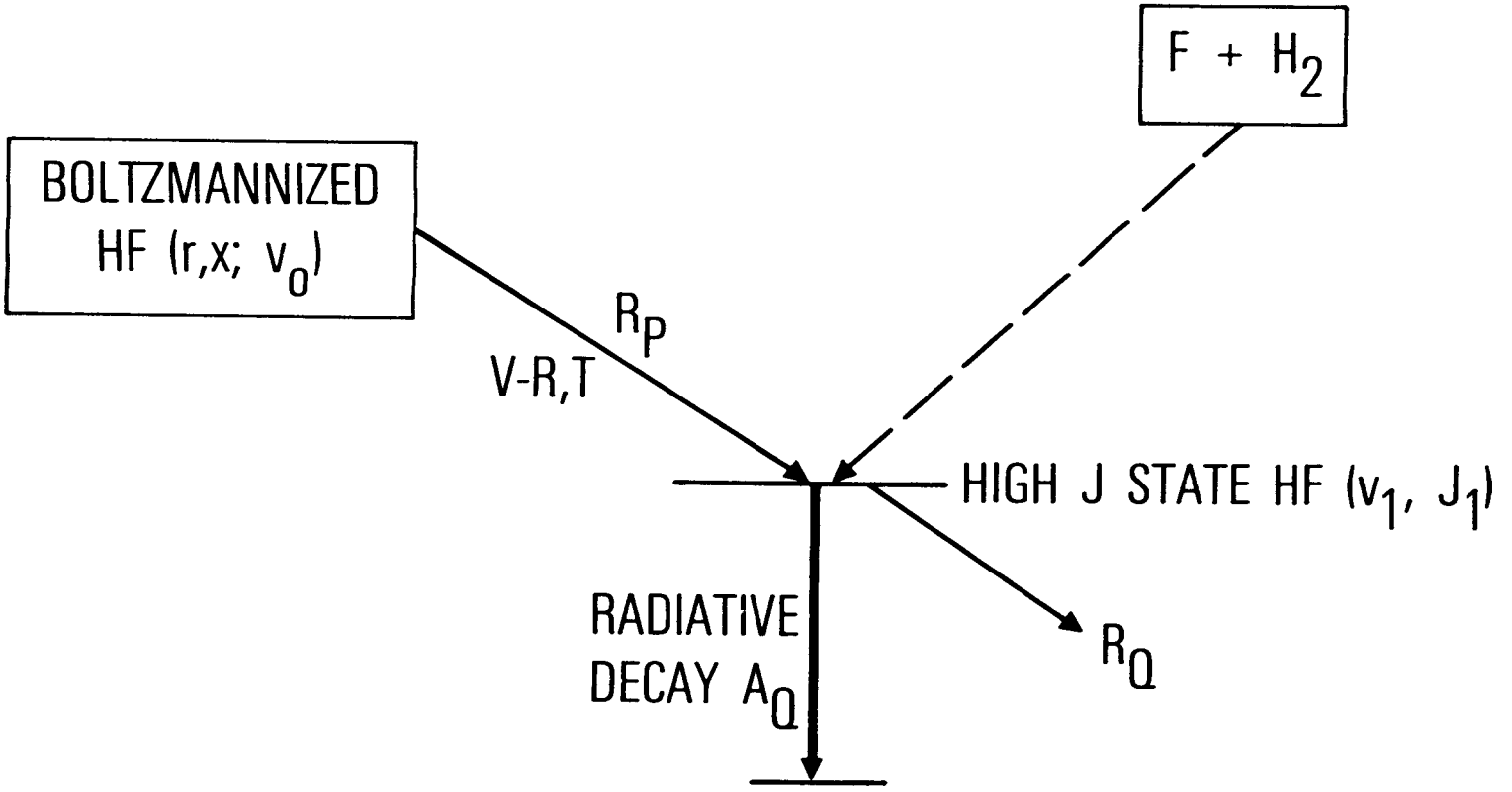

Fig. 8. Pathways in Density Model. R_P is the pumping rate by V-R,T transfer and R_Q, the collisional quenching rate.

Axial diffusion effects are observed but are considered to be not substantial for the first one and a half tube diameters downstream. Thus, diffusion effects are not included in this model. The use of Eqs. (11 and 12) and a systematic variation of K_p^{VR} and K_Q produces fits shown in Fig. 9. The models are particularly successful in simulating peak absolute number densities and peak location.

Although the product state has not appeared in classical trajectory calculations, it is conceptually and energetically possible that the v = 0, J = 22 state can be created by an H-atom exchange reaction

$$H + HF(v = 3, J) \rightarrow H + HF(v = 0, J = 22) \qquad (13)$$

Empirical quenching rates at 6×10^{13} cm^3 mol^{-1} sec^{-1} for H + HF(v = 3) have been reported to be over two orders of magnitude larger than those for lower v levels.[37,38,39] Originally it was suggested that this rate might consist of significant parts of the reverse of the abstraction reaction, exchange reaction, and V-R,T deactivation.[37,38] However, authors have shown in later experiments that the only pathway is the reverse to the chemical reaction F + H_2.[39] This view is further supported by the classical trajectory calculations,[40] which show collisional quenching rate coefficients not involving the reverse reaction to be less than order 10^{12} cm^3 mol^{-1} sec^{-1}. Further, the trajectory calculations do not predict such nearly resonant collisions as (Eq. 13) producing high J states to be highly probable. Any production rate of high J states portrayed by Eq. (13), at 10^{12} cm^3 mol^{-1} sec^{-1} rate coefficients and 10^{12} no-cm^{-3} H atom densities, would be too slow to be relevant on these flow tube time scales. Therefore, it is highly unlikely that any pathway such as Eq. (13) produces much v = 0, J = 22, and this process has not been included in the model.

D. MODEL RESULTS

Computed fits are compared with observed high J state densities in Fig. 9. Further fits of the low J state densities are shown in Fig. 7. Despite many parameters in the problem, the sensitivity of values R_p and R_Q to

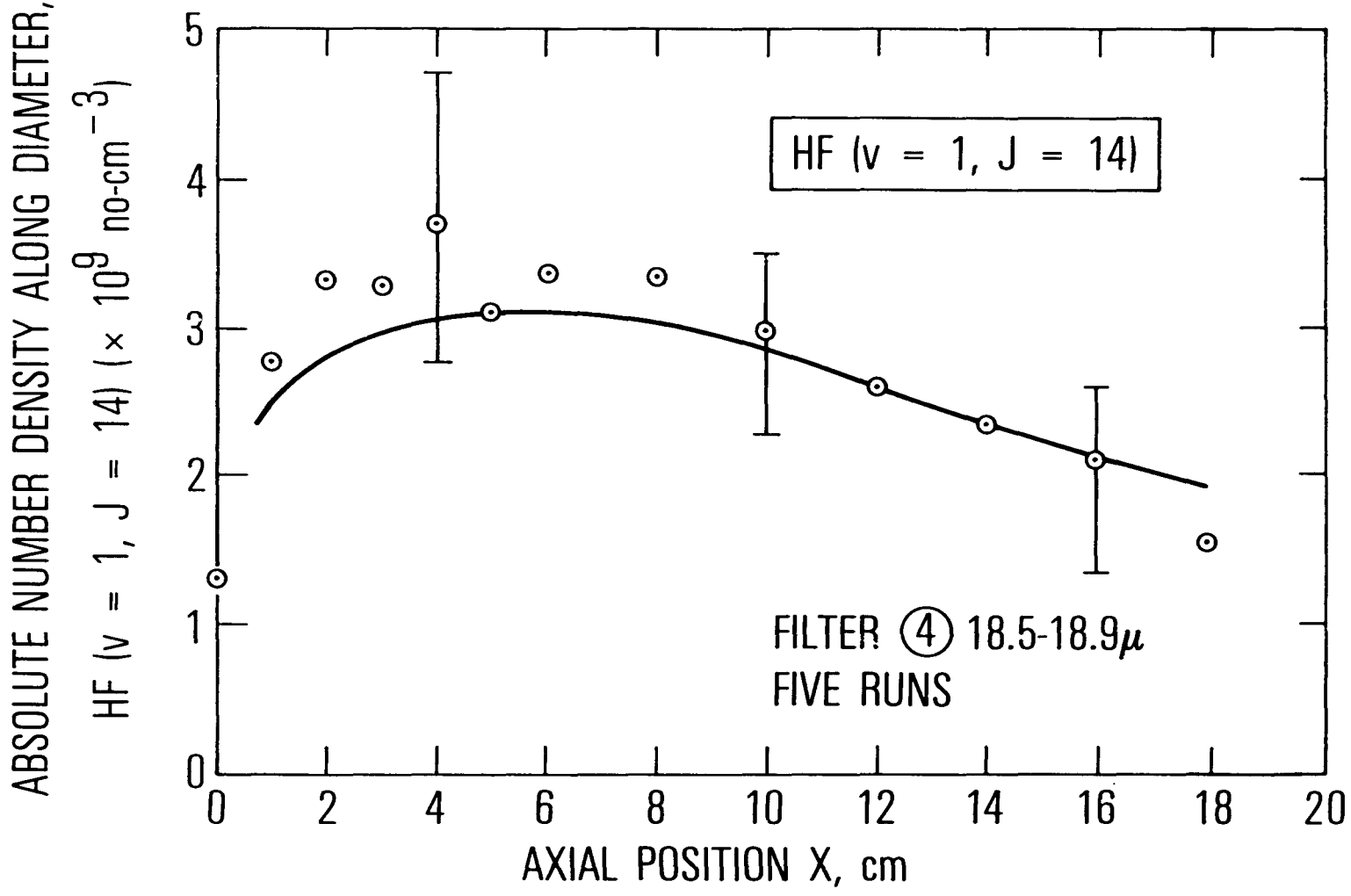

Fig. 9a. Model Fits of Two Experimental Cases. HF(1, 14) density as a function of tube axial position.

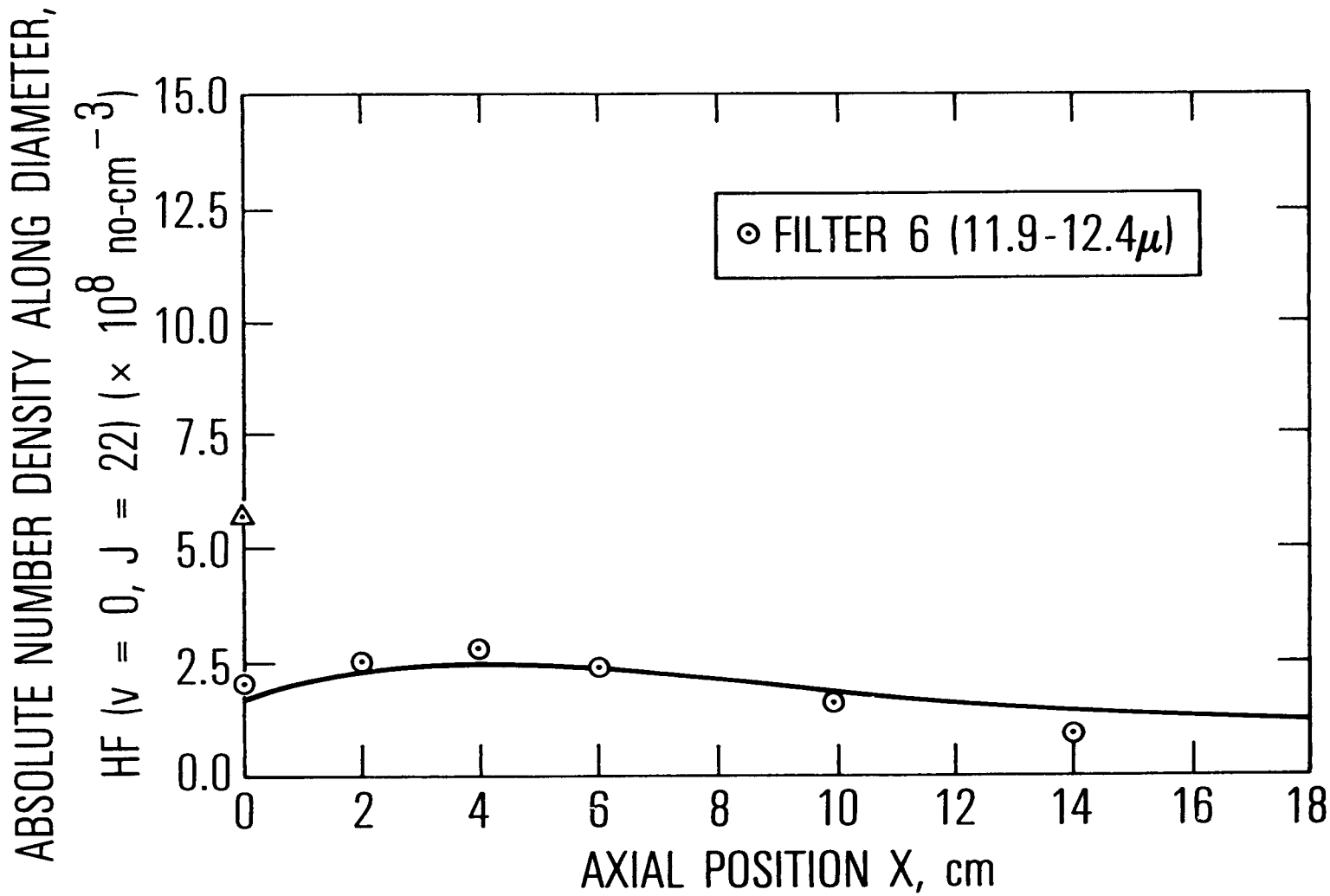

Fig. 9b. Model Fits of Two Experimental Cases. HF(0, 22) density as a function of tube axial position.

a specific solution is quite high, especially if the criteria of maximum absolute density, its axial locations, and decay as a function of axial location are all required. The curve fits are sufficiently successful to continue discussion.

In Table 4, the empirical pumping (R_P) and quenching (R_Q) rates needed for model fits of the data are displayed. If the pumping rates assume the forms for V-R transfer as previously assumed, the rate coefficients k^{VR} for V-R, where the collision partner is H_2, are $O(10^{10})$ cm^3 mol^{-1} sec^{-1}. Scaled by two orders of magnitude upward for HF collision partners, these V-R rate coefficients would range from 10^{12}-10^{13} cm^3 mol^{-1} sec^{-1}. These magnitudes are quite consistent with those rates in the work of Wilkins[1] for appearance of a density in a high J state from all possible low J states with higher v quantum numbers. There is also consistency in that the rate coefficient for a multiple v quantum process is smaller than that for a single v process.

The quenching rate includes radiative decay and collisional processes (Fig. 10). After the subtraction of the radiative processes, the collisional quenching rates remain quite large. If this quenching is caused only by V-R and R → V processes, the consequent state-to-state rate coefficients are 10 to 100 times those proposed by Wilkins[1] for HF collision partners! This result occurs because of the set pattern of β_i factors set forth for such processes in Table 3 with the HF partner as dominant. Thus, it does not seem plausible that these processes are the sole mechanisms in the quench.

The recent work of Thompson[27] suggests that another major quenching process is an R-T mechanism. In addition, R-R processes involving molecular collision partners such as H_2 and HF might also be included. The Thompson calculations show that state-to-state cross sections for R-T and V-R transfers can be large, on the order of 1 in 10 gas kinetic collisions, even with rare gas atoms such as argon as collision partners. The largest state-to-state R-T cross sections, for single quantum rotational quantum number changes, appear to be over an order of magnitude larger than those cross sections for V-R or R → V transfer. However, his calculations are all conducted at high relative translational energies above 0.2 eV with most of the work performed at 1.0 eV. An energy of 0.2 eV is equivalent to about 1600 cm^{-1} or an equivalent temperature around 2300 K. Thus, the current calculations would not detect any

Table 4. Kinetic Results from Model

	State	
	HF(0,22)	HF(1,14)
Fitted Pump Rate R_p (sec^{-1})	10.9	40.9
Fitted Quench Rate R_Q (sec^{-1})	8160	4590
Pumping Rate Coefficient		
K_{P1}^{VR} for M = H_2 (cm^3 mol^{-1} sec^{-1})	1.4×10^{10}	5.3×10^{10}
Scaled K_{P3}^{VR} for M = HF (cm^3 mol^{-1} sec^{-1})	1.4×10^{12}	5.3×10^{12}
	(3,J) → (0,22)	(2,J) → (1,14)
β_i: Case 1		
K_{Q1} for M = H_2 (cm^3 mol^{-1} sec^{-1})	1.0×10^{13}	5.6×10^{12}
Scaled K_{Q3} for M = HF (cm^3 mol^{-1} sec^{-1})	1.0×10^{15}	5.6×10^{14}
β_i: Case 2		
K_{Q2} for M = Ar (cm^3 mol^{-1} sec^{-1})	1.5×10^{11}	8.0×10^{10}
Scaled K_{Q3} for M = HF,H_2	1.5×10^{12}	8.0×10^{11}

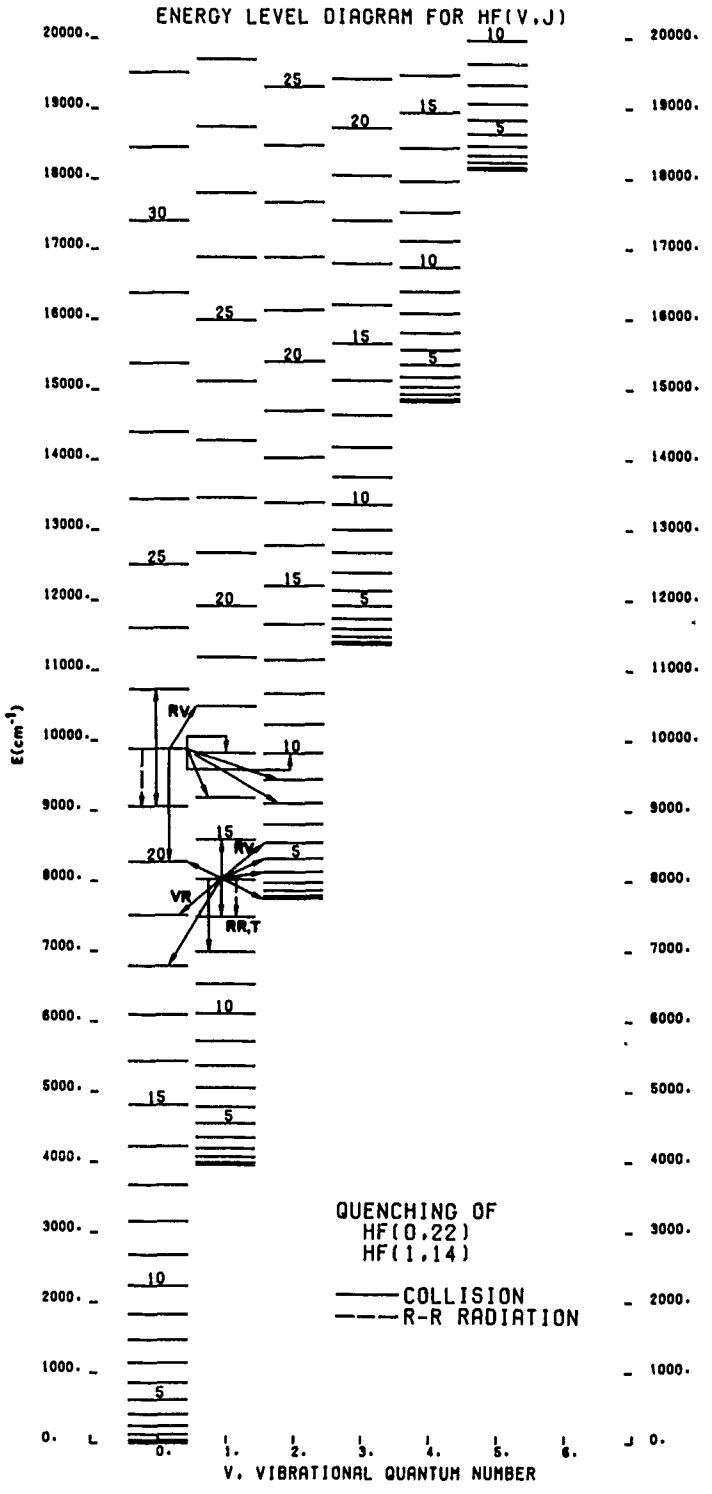

Fig. 10. Energy Level Diagram of HF Showing Quenching Processes for High J States

effects caused by energy spacings in the vibrational-rotational structure of HF or thermal effects caused by gas conditions at the low thermal energies of 300 K, 206 cm^{-1}, or 0.025 ev. There does seem to be a trend toward favoring R-T exoergic over endoergic collisional processes as the relative energy is reduced by Thompson, but the observation is not strongly conclusive.

In these experiments, the largest energy spacing is 819 cm^{-1} for v = 0, J = 22 to v = 0, J = 21. The available average thermal energy is one-fourth of this spacing. By Thompson's calculations, we might expect the T-R pathway from (0,22) to (0,23) to be not as important. The absolute values of cross-sections for a given pathway may also be significantly smaller because of this smaller thermal energy. Generally speaking, the higher the J state, the smaller the cross section, but the higher the J state, the significantly greater the number of exit pathways opened up for the v, J state. Exoergic $\Delta J = 1$ rotational relaxation by molecules is perhaps a factor of 10 faster than relaxation by atoms on the same pathway if the absolute cross sections recently reported by Wilkins and Kwok[41] for the HF chaperone are related to the calculations by Thompson.[27] Since the carrier gas is argon in these experiments, the high density of argon compared to reactive species makes the background gas the dominant chaperone for both rotational and vibrational relaxation, and R-T rotational relaxation the dominant form of relaxation.

In Table 4, if the quenching rates are interpreted as single path R-T mechanisms from J→J-1, one obtains state-to-state R-T rate coefficients for an argon chaperone of $O(10^{11})$ cm^3 mol^{-1} sec^{-1} or $O(10^{12})$ cm^3 $mol^{-1}sec^{-1}$ for H_2 or HF at presumed tenfold larger rate coefficients. If one further assumes that these rate coefficients vary in thermal energy with an $\exp(-\Delta E/kT)$ dependence, these coefficients can be scaled up to cases of high thermal energies, to cases with $\Delta E \ll kT$ scaled up to cases of high thermal energies, such as those computed by Thompson. One finds the scaled coefficients to be $O(10^{13})$ cm^3 mol^{-1} sec^{-1} and approaching $O(10^{14})$. Thus, our qualitative estimates and interpretations are quite consistent with the cross section calculations of both Thompson[27] and Wilkins.[41] The slightly larger value of K_Q for (0,22) can be a manifestation of the increased number of quenching paths with increased J or simply a variation in the pattern of the cross sections. Both possibilities are exhibited by Thompson's calculations.

V. CONCLUSIONS

Very high J states in HF(v, J) have been observed in a reactive fast flow in the large diameter flow tube. The observed behavior of these high J state absolute densities seems to support their production by collisional V-R processes from chemically produced and rotationally relaxed HF(v, J) species at much lower J. Modeling analysis of these experiments suggests that these observations are consistent with the theoretical works by Wilkins[1] and Thompson[27] for pumping high J states by V-R transfer, and by Thompson[27] and Wilkins[41] for quenching by R-T transfer and also consistent with the recent experimental efforts of Hinchen[19] and Haugen.[26]

Our work and these other efforts demonstrate that energy disposal in the internal energy manifold of the HF molecule by collisions depends on intricate relationships among what is generally considered as separate V-R and (R-R,T) and V-V classes of collisional transfer. The entire system can actually be viewed as a relaxation of internal energies to the equilibrium state by multiple pathways. Experimental insight into this complex relaxation system can be gained by working in regions of the system with large energy spacing, i.e., high J, at the lowest practical densities. One has a better chance of experimentally isolating state-to-state processes, which then can be compared with proposed theories.

Finally, we note that the methodologies of state preparation by chemical reaction combined with sophisticated emission detection techniques have permitted studies at very high J states not otherwise accessible. This capability has been achieved with the need for particular reagent species and an increase in the complexity of analysis caused by some lack of specificity in the chemical production of initial states.

REFERENCES

1. R. L. Wilkins, J. Chem. Phys. 67, 5838 (1977).

2. T. F. Deutsch, Appl. Phys. Lett. 11, 18 (1967).

3. D. P. Akitt and J. T. Yardley, IEEE J. Quan. Elec. QE-6, 113 (1970).

4. N. Skribanovitz, I. P. Herman, R. M. Osgood, Jr., M. S. Feld, and A. Javan, Appl. Phys. Lett. 20, 428 (1972).

5. H. Pummer and K. L. Kompa, Appl. Phys. Lett. 20, 356 (1972).

6. E. Cuellar, J. H. Parker, and G. C. Pimentel, J. Chem. Phys. 61, 422 (1974).

7. O. D. Krogh and G. C. Pimentel, J. Chem. Phys. 67, 2993 (1977).

8. E. Cuellar and G. C. Pimentel, J. Chem. Phys. 71, 1385 (1979).

9. E. R. Sirkin and G. C. Pimentel, J. Chem. Phys. 75, 604 (1981).

10. E. R. Sirkin and G. C. Pimentel, J. Chem. Phys. 77, 1314 (1982).

11. J. H. Smith and D. W. Robinson, J. Chem. Phys. 74, 5111 (1981).

12. G. D. Downey, D. W. Robinson, and J. H. Smith, J. Chem. Phys. 66, 1685 (1977).

13. J. H. Smith and D. W. Robinson, J. Chem. Phys. 68, 5474 (1978).

14. J. H. Smith and D. W. Robinson, J. Chem. Phys. 71, 271 (1979).

15. J. F. Bott, J. Chem. Phys. 70, 4123 (1979).

16. M. A. Kwok, unpublished.

17. P. R. Poole and I. W. Smith, J. Chem. Soc. Faraday Trans. II 73, 1434 (1977); 73, 1447 (1977).

18. L. S. Dzelzkalns and F. Kaufman, J. Chem. Phys. 77, 3508 (1982).

19. L. S. Dzelzkalns and F. Kaufman, J. Chem. Phys. 79, 3836 (1983).

20. J. J. Hinchen, private communication. Version published in Applied Atomic Collision Physics (Academic, New York, 1982), Vol. 3, p. 191. Also, J. J. Hinchen and R. H. Hobbs "Direct Measurements of Vibration-to-Rotation Population Transfer in HF" Paper ThI18, CLEO '84, Anaheim, CA (June 18-21, 1984).

21. D. J. Douglas and C. B. Moore, Chem. Phys. Lett. 57, 485 (1978).

22. J. K. Lampert, G. M. Jursich, and F. F. Crim, Chem. Phys. Lett. 71, 258 (1980).

23. G. M. Jursich and F. F. Crim, J. Chem. Phys. 74, 4455 (1981).

24. N. Cohen, M. A. Kwok, R. L. Wilkins, and J. F. Bott, "The Status of Rotational Nonequilibrium in HF Chemical Lasers," AIAA-83-1699, AIAA 16th Fluids and Plasma Dynamics Conference, also in Lasers in Fluid Mechanics and Plasmas Dynamics, ed. C. P. Wang (AIAA, New York, 1984), p. 81.

25. M. A. Kwok, E. F. Cross, and R. L. Wilkins, "In Search of High J States-in (HF(v) + M V-R Transfer." Tenth International Quantum Electronics Conference, Atlanta, May 29-June 1, 1978.

26. H. G. Haugen, W. H. Pence, and S. R. Leone, "Infrared Double Resonance Spectroscopy of V-T,R Relaxation of HF(v = 1): Direct Measurement of the High-J Populations," to be published.

27. D. L. Thompson, J. Chem. Phys. 76, 5947 (1982).

28. J. J. Hinchen and R. H. Hobbs, J. Chem. Phys. 65, 2732 (1976).

29. M. A. Kwok and N. Cohen, J. Chem. Phys. 61, 5221 (1975).

30. Frank J. Low, J.O.S.A. 51, 1300 (1961).

31. D. J. Benard, W. D. Slater, P. J. Love, and P. H. Lee, Appl. Optics 16, 2108 (1972).

32. J. C. Polanyi and D. C. Tardy, J. Chem. Phys. 51, 5717 (1969).

33. R. L. Wilkins, J. Chem. Phys. 57, 912 (1972).

34. J. P. Sung and D. W. Setser, J. Chem. Phys. 69, 3868 (1978).

35. N. Cohen and J. F. Bott, Handbook of Chemical Lasers, Ch. 2, Kinetics of Hydrogen Halide Chemical Lasers, J. Wiley, N.Y., 1976, p. 65.

36. R. F. Heidner and J. F. Bott, J. Chem. Phys. 63, 1810 (1975).

37. J. F. Bott and R. F. Heidner III, J. Chem. Phys. 66, 2878 (1977).

38. J. F. Bott and R. F. Heidner III, J. Chem. Phys. 68, 1708 (1978).

39. F. E. Bartoszek, D. M. Manas, and J. C. Polanyi, J. Chem. Phys. 69, 933 (1978).

40. R. L. Wilkins, J. Chem. Phys. 58, 3038 (1972).

41. R. L. Wilkins and M. A. Kwok, J. Chem. Phys. 78, 7153 (1983).

APPENDIX A: SPECTROSCOPY

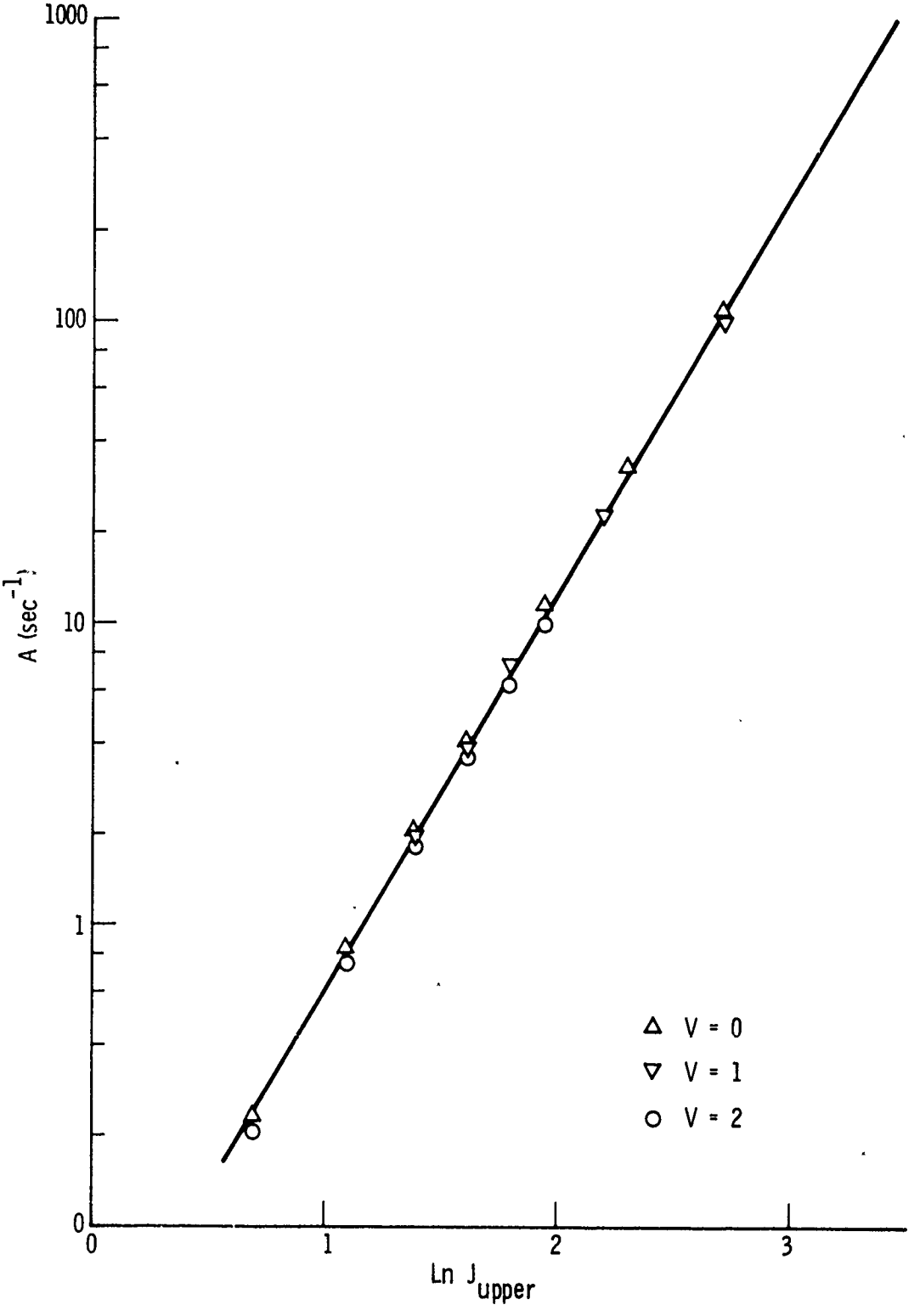

Fig. A-1. Einstein Coefficients for HF Rotational-Rotational Transitions. v = 0 or v = 1. J^3 dependence can be seen.

APPENDIX B: BOLOMETER CALIBRATION

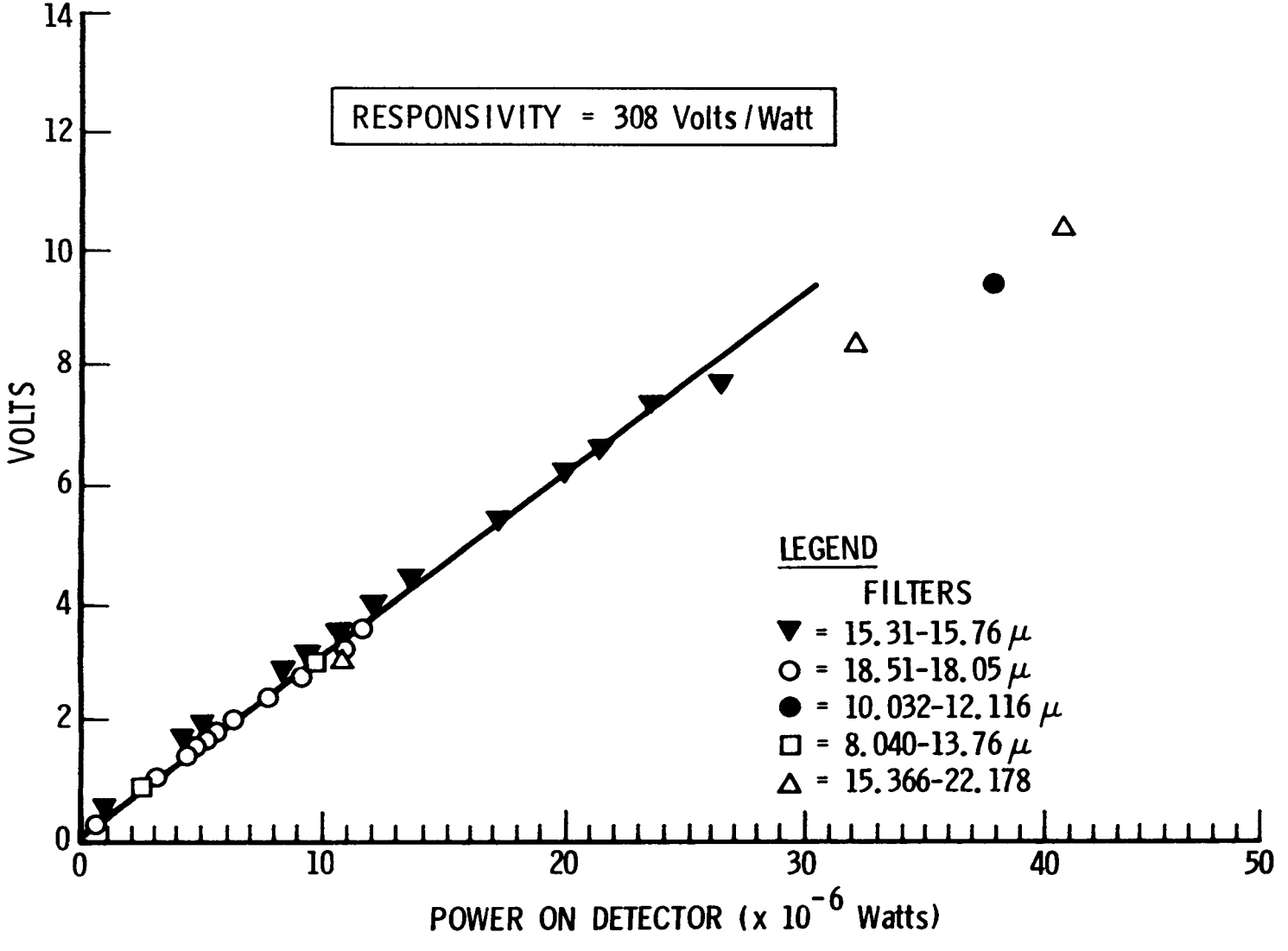

Fig. B-1. Germanium Bolometer Calibration

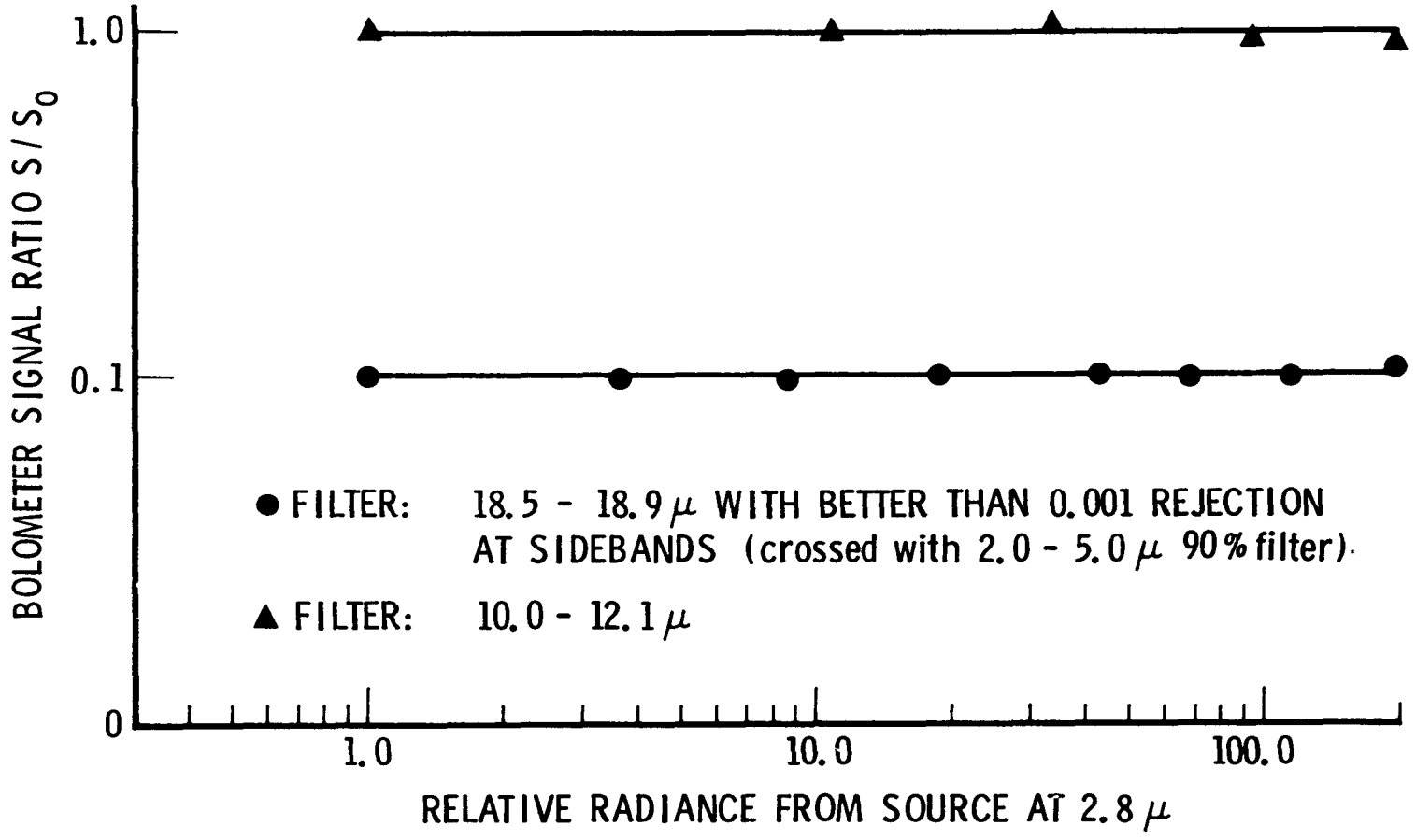

Fig. B-2. Typical Filter Sideband Leakage Measurements at 2.5 to 3.1 μ

☆ U.S. GOVERNMENT PRINTING OFFICE: 1985-585-660/436

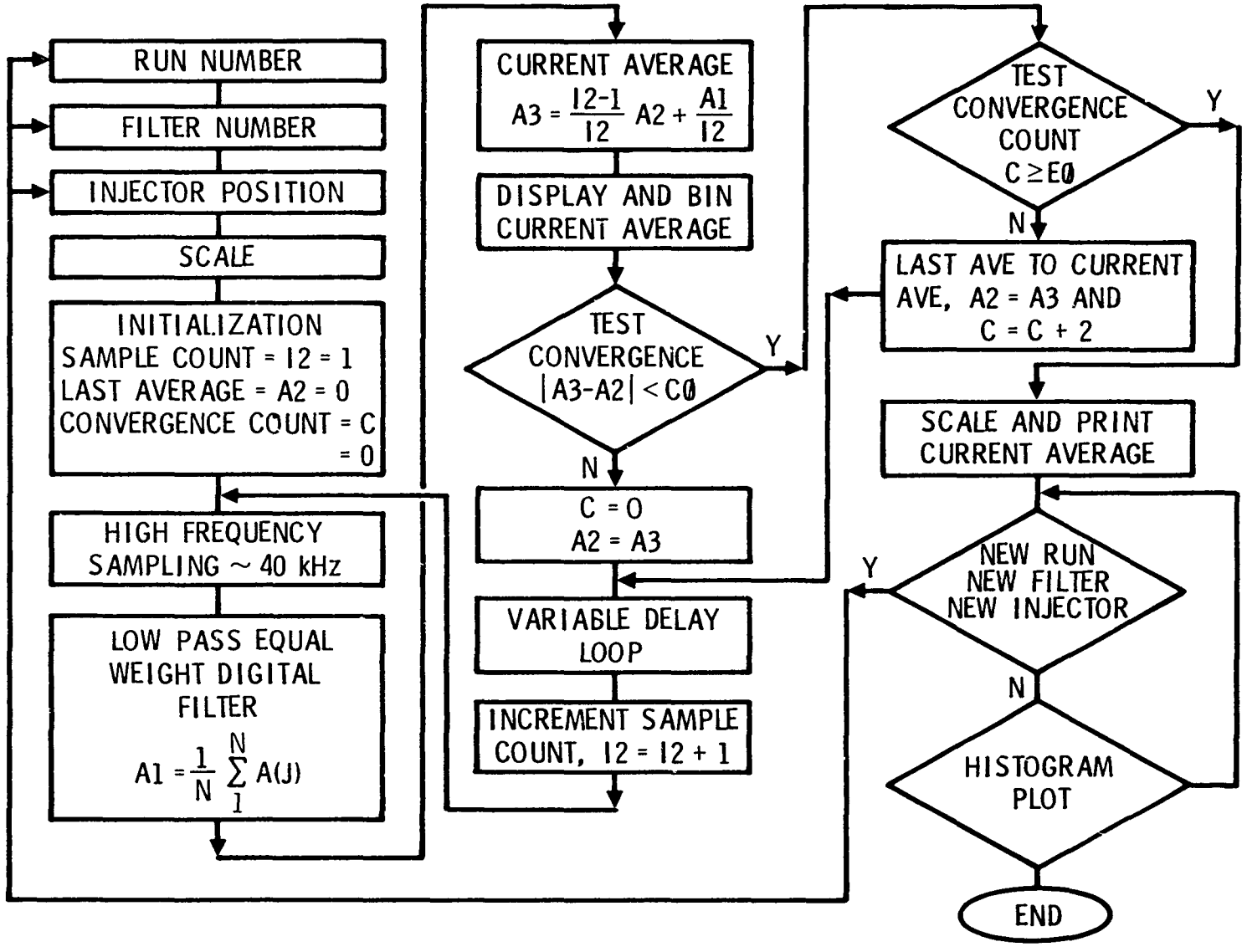

Fig. B-3. Flow Chart for Software Development of Digital Filtering and Signal Averaging of Bolometer-Lock-in Amplifier Signals

LABORATORY OPERATIONS

The Laboratory Operations of The Aerospace Corporation is conducting experimental and theoretical investigations necessary for the evaluation and application of scientific advances to new military space systems. Versatility and flexibility have been developed to a high degree by the laboratory personnel in dealing with the many problems encountered in the nation's rapidly developing space systems. Expertise in the latest scientific developments is vital to the accomplishment of tasks related to these problems. The laboratories that contribute to this research are:

Aerophysics Laboratory: Launch vehicle and reentry fluid mechanics, heat transfer and flight dynamics; chemical and electric propulsion, propellant chemistry, environmental hazards, trace detection; spacecraft structural mechanics, contamination, thermal and structural control; high temperature thermomechanics, gas kinetics and radiation; cw and pulsed laser development including chemical kinetics, spectroscopy, optical resonators, beam control, atmospheric propagation, laser effects and countermeasures.

Chemistry and Physics Laboratory: Atmospheric chemical reactions, atmospheric optics, light scattering, state-specific chemical reactions and radiation transport in rocket plumes, applied laser spectroscopy, laser chemistry, laser optoelectronics, solar cell physics, battery electrochemistry, space vacuum and radiation effects on materials, lubrication and surface phenomena, thermionic emission, photosensitive materials and detectors, atomic frequency standards, and environmental chemistry.

Computer Science Laboratory: Program verification, program translation, performance-sensitive system design, distributed architectures for spaceborne computers, fault-tolerant computer systems, artificial intelligence and microelectronics applications.

Electronics Research Laboratory: Microelectronics, GaAs low noise and power devices, semiconductor lasers, electromagnetic and optical propagation phenomena, quantum electronics, laser communications, lidar, and electro-optics; communication sciences, applied electronics, semiconductor crystal and device physics, radiometric imaging; millimeter wave, microwave technology, and RF systems research.

Materials Sciences Laboratory: Development of new materials: metal matrix composites, polymers, and new forms of carbon; nondestructive evaluation, component failure analysis and reliability; fracture mechanics and stress corrosion; analysis and evaluation of materials at cryogenic and elevated temperatures as well as in space and enemy-induced environments.

Space Sciences Laboratory: Magnetospheric, auroral and cosmic ray physics, wave-particle interactions, magnetospheric plasma waves; atmospheric and ionospheric physics, density and composition of the upper atmosphere, remote sensing using atmospheric radiation; solar physics, infrared astronomy, infrared signature analysis; effects of solar activity, magnetic storms and nuclear explosions on the earth's atmosphere, ionosphere and magnetosphere; effects of electromagnetic and particulate radiations on space systems; space instrumentation.